The mechanism of improved aeration due to gas films on leaves of submerged rice

Pieter Verboven[1,*], Ole Pedersen[2,3,4], Quang Tri Ho[1], Bart M. Nicolai[1], and Timothy D. Colmer[3]

[1]Division BIOSYST-MeBioS, University of Leuven, Willem de Croylaan 42, 3001 Leuven, Belgium.

[2]Freshwater Biological Laboratory, Institute of Biology, University of Copenhagen, Universitetsparken 4, 3rd floor, 2100 Copenhagen, Denmark.

[3]School of Plant Biology and the Institute of Agriculture, The University of Western Australia, 35 Stirling Highway, Crawley, WA 6009, Australia.

[4]Institute of Advanced Studies, The University of Western Australia, 35 Stirling Highway, Crawley, WA 6009, Australia.

***Corresponding author:** Pieter Verboven

Tel: +32 16 321453; **E-mail:** pieter.verboven@biw.kuleuven.be

Running head: *Leaf gas films on submerged rice*

Number of figures: 13; **Number of tables:** 1

Abstract

Some terrestrial wetland plants, such as rice, have super-hydrophobic leaf surfaces which retain a gas film when submerged. O_2 movement through the diffusive boundary layer (DBL) of floodwater, gas film and stomata into leaf mesophyll was explored by means of a reaction-diffusion model that was solved in a 3D leaf anatomy model. The anatomy and dark respiration leaves of rice (*Oryza sativa* L.) were measured and used to compute O_2 fluxes and partial pressure of O_2 (pO_2) in the DBL, gas film and leaf when submerged. The effects of floodwater pO_2, DBL thickness, cuticle permeability, presence of gas film and stomatal opening were explored. Under O_2-limiting conditions of the bulk water (pO_2 < 10 kPa), the gas film significantly increases the O_2 flux into submerged leaves regardless of whether stomata are fully or partly open. With a gas film, tissue pO_2 substantially increases, even for the slightest stomatal opening, but not when stomata are completely closed. The effect of gas films increases with decreasing cuticle permeability. O_2 flux and tissue pO_2 decrease with increasing DBL thickness. The present modelling analysis provides a mechanistic understanding of how leaf gas films facilitate O_2 entry into submerged plants.

Key words: flooding stress, leaf hydrophobicity, leaf respiration, submergence tolerance, modelling, tissue hypoxia, plant aeration, tissue porosity, leaf gas exchange, *Oryza sativa*

Introduction

Submergence is a severe abiotic stress for terrestrial plants. Floods resulting in submergence impact on natural plant communities (Bailey-Serres & Voesenek 2008) and are also a constraint in some areas used for cultivation of lowland rice (Widawsky & O'Toole 1990; Zeigler & Puckridge 1995). Submergence greatly restricts O_2 uptake from the environment as diffusion is 10,000 times slower in water than in air (Armstrong 1979). During the day, photosynthesis by submerged leaves produces O_2; whereas at night, the only source of O_2 to the leaves is that dissolved in the water (Sand-Jensen *et al.* 2005; Winkel *et al.* 2013). O_2 produced by photosynthesis during day time or diffusing into the leaves from the water during night time sustains respiration in leaves, and also a portion of this O_2 moves via rapid gas-phase diffusion within the aerenchyma to the roots. However, even with internal movement of O_2 within submerged plants to roots in anoxic substrates, these tissues can still suffer O_2 deficits (Waters *et al.* 1989; Pedersen *et al.* 2006; Winkel *et al.* 2013). Leaf traits that promote gas exchange with floodwaters enhance entry of O_2 for respiration during the night, and of CO_2 for underwater photosynthesis during the day (Mommer & Visser 2005; Colmer *et al.* 2011).

Leaves of aquatic plants are adapted for underwater gas exchange (Sculthorpe 1967; Maberly & Madsen 2002) and some terrestrial wetland plants produce new acclimated leaves with enhanced gas exchange under water (Nielsen & Sand-Jensen 1989; Mommer & Visser 2005). Other terrestrial wetland plants, for example rice, have super-hydrophobic leaf surfaces which retain a gas film when submerged, a feature which facilitates underwater gas exchange (Raskin & Kende 1983; Colmer & Pedersen 2008b). The enhancement of leaf CO_2 and O_2 exchange by gas films when under water, and the

67 resulting influence on internal aeration of submerged plants, have been demonstrated
68 (Beckett & Armstrong 1992; Armstrong *et al.* 1994; Pedersen *et al.* 2009; Winkel *et al.*
69 2011). The mechanism of this improved underwater gas exchange resulting from leaf gas
70 films with characteristics of stomata, cuticle permeability and diffusive boundary layer
71 (DBL) is explored in detail in the present study.
72
73 Leaf tissue O_2 status when submerged is determined by both environmental conditions and
74 leaf properties. When in darkness of night, the key factors include: (i) the O_2
75 concentration, flow conditions and temperature in the water, (ii) the total resistance to
76 diffusion from the bulk medium into the leaves (DBL distance, surface gas films, cuticle
77 resistance and stomatal resistance), (iii) internal tissue resistance (path length, gas-filled
78 pores and their connectivity), and (iv) tissue respiration rate. Here, we focus on the role of
79 leaf gas films in the enhancement of O_2 entry into submerged leaves of rice. Empirical
80 measurements have shown that the presence of gas films reduced by about 5-times the
81 apparent resistances for O_2 entry into submerged leaves when in darkness (*Phargmites*
82 *australis*, Colmer & Pedersen 2008b) and for CO_2 entry when in light (*Oryza sativa*,
83 Pedersen *et al.* 2009). The improved underwater gas exchange afforded by the gas films
84 on leaves was, in analogy with the functioning of surface gas layers on some aquatic
85 insects, suggested to result from a large gas-to-water interface (Raskin & Kende 1983;
86 Setter *et al.* 1989; Colmer & Pedersen 2008b; Pedersen *et al.* 2009; Pedersen & Colmer
87 2012) and rapid gas-phase diffusion within the films to open stomata (suggested by
88 Colmer & Pedersen 2008b). By contrast, for leaves without gas films Mommer & Visser
89 (2005) suggested that the stomata might close upon submergence so that CO_2 and O_2 must
90 then transverse the cuticle (Mommer *et al.* 2004); even if stomata were open, leaves

lacking gas films would have a much smaller area of gas-to-aqueous phase surface interface (i.e. only at the stomata, so < 1/100th of the interface with gas films present). Whether stomata are open or closed would presumably also be determined by the light environment, and may thus differ between daytime (open) and night (closed). Stomatal closure may be incomplete at night (Caird *et al.* 2007), and therefore partial closure effects may also occur or even be more relevant.

Here, we used three-dimensional diffusion modelling of O_2 (Verboven *et al.* 2012) entry into a simulated rice leaf lamina in darkness to test three key hypotheses as related to gas film functioning in O_2 consumption and tissue concentrations of submerged leaves, and also assessed these in contrasting environmental conditions. (1) The presence of gas films reduces the resistance to O_2 entry into submerged leaves. (2) When gas films are present, O_2 would move in a perpendicular path through the aqueous (slow) diffusive boundary layer (DBL) into the gas film and (fast in the gas phase) to open or partially closed stomata; whereas, without gas films, O_2 would predominately follow oblique paths (longer) through the aqueous DBL to the stomata (suggested by W. Armstrong; in Colmer *et al.* 2014). (3) Stomatal closure will largely negate the beneficial effects of leaf gas films on underwater gas exchange, as then O_2 would need to enter across the cuticle which poses high resistance. The contrasting conditions under which these hypotheses were tested included the effects of different DBL thickness (as would be influenced by, e.g., flowing waters), different O_2 partial pressure (pO_2) in the water (e.g., as in diurnal cycles in floodwaters) and different cuticle permeability.

Materials and methods

Plant materials

Oryza sativa L. var. Amaroo was raised in aerated nutrient solution (composition in Colmer & Pedersen 2008a), and then pre-treated for the final 7 days in de-oxygenated stagnant 0.1% (w/v) agar in the nutrient solution of otherwise same composition, with shoots remaining in air, prior to use in the experiments. The ages of plants used varied from 6-8 weeks, by which time the plants had tillered and the lengths of mature leaves (including the sheath) were 40-50 cm long.

Respiration of lamina segments under water

Lamina segments of approximately 30 mm length were taken half-way between the ligule and tip of the youngest fully expanded leaf. Dark respiration of each replicate segment was measured in a microrespiration system (MicroResp, Unisense A/S, Aarhus, Denmark) in darkness at 30 °C. The chambers were full of artificial floodwater following the recipe of Pedersen *et al.* (2009) and these submerged lamina segments possessed gas films. Measurements were taken using 4 mL glass chambers with a capillary hole in the glass stopper (MR Ch-4000, Unisense A/S, Aarhus, Denmark) through which an O_2 microelectrode (OX-MR, Unisense A/S, Aarhus, Denmark) was inserted. The medium used was a general purpose artificial floodwater solution based on Smart & Barko (1985); see Colmer & Pedersen (2008b) and Pedersen *et al.* (2013) for further details.

Microelectrode profiling of pO_2 gradients towards lamina segments under water in the dark

For each replicate, one lamina segment of ~ 60 mm length was taken half-way between the ligule and tip of the youngest fully expanded leaf. The segment was mounted on

double-sided adhesive tape in a Petri dish that was filled with artificial floodwater (for composition see Pedersen *et al.* 2009); this was required to ensure no movement of the sample, but would have restricted O_2 uptake via the lower surface and therefore likely resulted in greater O_2 uptake via the exposed upper surface than if both sides were exposed to the bulk medium. This arrangement enabled us to achieve our aim to obtain profiles adequate for the purpose to estimate dimensions of the surface gas layer and an approximation of the DBL distance; for considerations of tissue O_2 consumption we use data obtained for excised lamina in well-stirred cuvettes with both leaf sides exposed (see previous sub-heading in this Materials and Methods). Convection in the water was standardized by blowing a gentle stream of air (Pasteur pipette connected to an air pump) across the water surface. An O_2 microelectrode (tip diameter = 10 µm, OX-10, Unisense A/S, Aarhus, Denmark) was mounted on a motor driven micromanipulator (MM33, Unisense A/S, Aarhus, Denmark) driving the electrode towards the leaf surface at 20 µm steps, starting in the bulk medium ~ 1000 µm above the leaf surface. The O_2 microelectrode was connected to a pA meter (Unisense Multimeter, Unisense A/S, Aarhus, Denmark) and signal was collected on a laptop computer using Sensortrace Pro (Unisense A/S, Aarhus, Denmark). All measurements were carried out in darkness at 30 ºC. The DBL thickness was calculated from the pO_2 gradients in the medium, according to Jørgensen & Revsbech (1985).

Lamina characteristics

External gas film volume and tissue porosity (% gas volume per unit tissue volume) were measured for lamina segments of ~ 60 mm length taken half-way between the ligule and tip of the youngest fully expanded leaf and cut longitudinally to remove the central mid-

rib tissue. The procedure involved determining tissue buoyancy before and after gas film removal (for details see Colmer & Pedersen 2008b) and then also after vacuum infiltration of the tissue gas spaces with water, using the method of Raskin (1983) with equations as modified by Thomson *et al.* (1990). The gas film thickness was estimated by relating the gas film volume to total leaf surface area (i.e. both sides). The resulting parameters are given in Table 1.

The stomatal patterns of arrangement and density per unit leaf area were measured on surface impressions of the lamina obtained by painting enamel nail polish onto the surface and then stripping it off when dry. These impressions were viewed under magnification (Axioskop 2, Zeiss, Germany) and images were captured using a digital camera. Stomata numbers were counted and distances between adjacent stomata (both across and along the lamina) were measured using ImageJ (Schneider *et al.* 2012). Leaf thickness was measured on transverse sections of lamina, using the same microscope equipped with a digital camera as described above, and analyses of distances of tissues on the calibrated images.

All measured parameters, as well as other parameters for rice leaves taken from published papers and used for modelling (see next section), are given in Table 1.

Simulation model of leaf gas-exchange under water (O_2 entry into lamina of submerged leaves in the dark)

Different configurations of submerged leaves (lamina) were studied taking into account the DBL, the gas film if present, stomatal opening, and cuticle permeability, as influencing

O_2 diffusion into respiring, submerged leaves in the dark (Figure 1). The O_2 movement from water to submerged leaves in darkness was modelled using a 3D diffusion-reaction model (Ho *et al.* 2011) to describe O_2 diffusion and consumption in the water-leaf system to predict pO_2 profiles and diffusion fluxes. The aim of the model was to explain the effect of the DBL in the water, the presence of the gas film, cuticle permeability, and the stomatal aperture (i.e., open, almost closed, closed) on the rate of O_2 uptake by, and internal pO_2 of the submerged leaf.

A 3D geometrical model of the lamina of a rice leaf was constructed. Assuming symmetry of abaxial and adaxial sides verified by similar stomatal density (Table 1), only the adaxial half of the leaf was modelled (Figure 2). Stomata on rice leaf lamina occur in repetitive line patterns with typical in-line and line-to-line distances given in Table 1. A representative leaf area sample was thus chosen that contains two stomata, with symmetry through the cut planes. One cut plane was through the middle of the stomata, revealing the substomatal cavity that is assumed to be a half sphere in the model. The other cut plane was halfway in between stomata through the mesophyll. The resulting porosity of the model lamina, taking into account the cavity and a mesophyll porosity of 2%, was 5%; this value corresponds to the range of observations (Table 1), but whole leaves with mid-rib have a higher total porosity (Colmer & Pedersen 2008a).

The length of the stomatal opening was identified on micrographs and the width of the open stomata was assumed to be 1.1 µm (Ishihara *et al.* 1971), resulting in 0.37% of the leaf surface area when all stomata are fully opened. Fractional closure of the stomata was assumed to result in reduction of the opening, whereas at 5% opening a small aperture in

the middle of each stoma is left open, equal to a total open area of the leaf surface of less than 0.02% (Table 1). The resulting 3D geometrical model used on the simulations is plotted in Figure 2.

The model distinguished: (1) the free flowing water with uniform pO_2, (2) the DBL with specified thickness between 45 and 370 µm, (3) the gas film with specified thickness of 60 µm, (4) the epidermis cell layer of 10 µm with cuticle, (5) the stomatal opening with varying open area, (6) the substomatal cavity and (7) the leaf mesophyll. The considered half leaf thickness was 58 µm and the bulk mesophyll porosity was 2%. O_2 diffusion coefficient values were applied to the different parts according to whether diffusion takes place in gas, water or porous tissue (Table 1). The diffusion coefficient of mesophyll was assumed to be equal to the porosity times the diffusion coefficient in air (Ho *et al.* 2009), assuming a well-connected airspace throughout the mesopyll such that the tortuosity is 1. The O_2 permeability of the cuticle was implemented as a boundary transfer coefficient between the external environment and internal parts of the leaf (Lendzian 1982; Lendzian & Kertiens 1991; Frost-Christensen *et al.* 2003). Spatial variations and anisotropy of the O_2 diffusion properties within tissues were neglected.

Leaf O_2 consumption was modelled by means of a Michaelis-Menten equation with maximum consumption rates in each tissue equal to measured rates (Table 1). The mitochondrial K_{M,O_2} value was assumed to be equal to 0.148 µM (0.0108 kPa) (Ho *et al.* 2009; Armstrong & Beckett 2011a).

234 The 3D model was developed and solved using the finite element method in COMSOL
235 3.5a (Comsol B.V., Stockholm, Sweden). The model is written as follows, for steady state
236 gas exchange:

237 $$0 = \nabla \cdot D^{i}_{O_2,g} \nabla[\mathrm{O_2}]_g + V_{O_2} \qquad (1)$$

238 with ∇ (m^{-1}) the gradient operator, $[O_2]_g$ (mol m^{-3}) the gaseous O_2 concentration, $D^{i}_{O_2,g}$
239 (m^2 s^{-1}) the gaseous diffusion coefficient of O_2 in compartment *i* of the model (with *i*:
240 mesophyll, epidermis, gas film or DBL), and R_{O_2} (mol m^{-3} s^{-1}) the consumption rate of O_2.

241

242 We assume that equilibrium between water and gas layers is established. At equilibrium,
243 the relationship between the O_2 concentration in the gas phase $[O_2]_g$ and that in the water
244 $[O_2]_l$ is given by Henry's law (Ho *et al.* 2009):

245 $$[\mathrm{O_2}]_l = R \cdot T \cdot H_{O_2} \cdot [\mathrm{O_2}]_g \qquad (2)$$

246 with R (J mol^{-1} K^{-1}) the universal gas constant, T temperature (K) and H_{O_2} the Henry
247 constant for water.

248

249 If the model is to use a gas-phase O_2 concentration as the source then account has to be
250 taken of the approximately 30-fold drop in concentration across the air-water interface.
251 This also effectively increases the diffusive resistance through the water by a factor 30 (~
252 $R \cdot T \cdot H_{O_2}$). We use equation (2) to express the diffusion flux J_{O_2} (mol m^{-2} s^{-1}) through
253 water layers in gas-equivalent formulation:

254 $$J_{O_2} = D^{i}_{O_2,l} \nabla[\mathrm{O_2}]_l = D^{i}_{O_2,l} \cdot R \cdot T \cdot H_{O_2} \nabla[\mathrm{O_2}]_g = D^{i}_{O_2,g} \nabla[\mathrm{O_2}]_g \qquad (3)$$

The gas-based diffusivity values $D^{i}_{O_2,g}$ of the different layers can be directly compared to assess ratios of resistances of the different layers. For example, the diffusion coefficient in water (2.75×10^{-9} m^2 s^{-1}) converts to a value on gas concentration basis equal to 9.3×10^{-11} m^2 s^{-1} and thus is 5 orders of magnitude smaller than that of air (2.15×10^{-5} m^2 s^{-1}).

The cuticle is essentially a thin barrier for gas exchange. Passive gas transfer across the cuticle is comparative to Fick's first law as a consequence of a concentration difference over the cuticle. The flux J_{O_2} (mol m^{-2} s^{-1}) through the cuticle was written as:

$$J_{O_2} = -P_{O_2,g}\Delta[O_2]_g \qquad (4)$$

with $P_{O_2,g}$ (m s^{-1}) the permeability of the cuticle. Experimentally determined permeability values provided in other works (Lendzian 1982; Lendzian & Kertiens 1991; Frost-Christensen *et al.* 2003) were calculated on water phase basis. The corresponding range of average permeability in gas phase was 1×10^{-8} to 5.2×10^{-7} m s^{-1} covering the lower end of the range of cuticles of leaves of *Citrus aurantium* L., fruits of *Lycopersicon esculentum* L. and *Capsicum annuum* L., and in the higher end of the range aerial leaves of amphibious plants. Two values in the range were used for direct comparison of resulting O_2 fluxes and pO_2 profiles: 1×10^{-8} m s^{-1} and 3.45×10^{-7} m s^{-1}. A more elaborate sensitivity analysis is performed in supplementary material.

Outside the leaf, the respiration V_{O_2} (mol m^{-3} s^{-1}) is zero while in the tissue this term is the consumption rate of the O_2. According to Michaelis–Menten kinetics, the following equation can be used (Lammertyn *et al.* 2001):

277 $$V_{O_2} = -\frac{V_{\max,O_2} \cdot [O_2]_g}{K_{M,O_2} + [O_2]_g} \quad (5)$$

278 with $V_{\max,O_2}$ (mol m^{-3} s^{-1}) the maximum respiration rate and K_{M,O_2} (mol m^{-3}) the

279 Michaelis-Menten constant.

280

281 **Data analyses**

282 GraphPad Prism 6 (GraphPad Software Inc., http://www.graphpad.com) was used for

283 fitting a Michaelis-Menten model to the dark respiration data. 3D contour and vector plots

284 of O_2 concentrations and fluxes in the water-leaf gas film-lamina tissue system were

285 rendered in Comsol 3.5a (Comsol B.V., Stockholm, Sweden).

286

287 The increase in resistance to O_2 flow into the leaf by absence of the gas film is quantified

288 by calculating the ratio of flow resistance of cases without gas film to that of

289 corresponding cases with the gas film. For each case, the O_2 flux from bulk water to leaf

290 tissue equals the diffusion through the DBL:

291 $$J_{O_2} = -1/R_{O_2,g}\left([O_2]_{g,bulk} - [O_2]_{g,tissue}\right) = -D^w_{O_2,g}\frac{\Delta[O_2]_{g,DBL}}{\Delta L_{DBL}} \quad (6)$$

292 with $R_{O_2,g}$ [s m^{-1}] the total resistance and $\Delta[O_2]_{g,DBL} / \Delta L_{DBL}$ the concentration gradient in

293 the DBL. The ratio of fluxes for cases without gas film (-GF) to cases with gas film (+GF)

294 $\left(J_{O_2}\right)_{-GF} / \left(J_{O_2}\right)_{+GF}$ can be rearranged to obtain the resistance ratio $r_{R_{O_2}}$:

295 $$r_{R_{O_2}} = \frac{\left(R_{O_2,g}\right)_{-GF}}{\left(R_{O_2,g}\right)_{+GF}} = \frac{\left([O_2]_{g,bulk} - [O_2]_{g,tissue}\right)_{-GF}}{\left([O_2]_{g,bulk} - [O_2]_{g,tissue}\right)_{+GF}} \frac{\left(\Delta[O_2]_{g,DBL} / \Delta L_{DBL}\right)_{+GF}}{\left(\Delta[O_2]_{g,DBL} / \Delta L_{DBL}\right)_{-GF}} \quad (7)$$

296 Partial pressure of O_2, pO_2 [kPa], is calculated from $[O_2]_g$, using the universal gas law and
297 further used in this paper.
298
299 **Results**
300 **Dark respiration rate of lamina of rice leaves**
301 Figure 3 plots the measured and fitted dark respiration curve of the submerged rice lamina
302 segments. Respiratory fluxes decrease with decreasing pO_2 in the bulk water. The
303 Michaelis-Menten constant, i.e. apparent K_m value, of the fitted respiration model is 3.08
304 kPa, and clearly exceeds that of isolated mitochondria (a value of 0.0108 kPa was
305 measured on soybean, (Millar *et al.* 1994). Such response has been observed in respiration
306 measurements of other plant organs, such as roots and fruits (Zabalza *et al.* 2009;
307 Armstrong & Beckett 2011a; Ho *et al.* 2011). The maximum respiration rate corresponds
308 to 0.012 mol O_2 m^{-3} s^{-1}, expressed on a tissue volume basis using leaf dimensions given in
309 Table 1. This value was used in the simulations.
310
311 **Oxygen profiles observed on rice leaves are affected by gas film presence and**
312 **stomatal opening**
313 Figure 4 presents a measured pO_2 profile into the lamina of a submerged rice leaf with a
314 gas film, when in darkness. The largest drop in O_2 concentration is observed across the
315 DBL from the well mixed bulk water to the gas film on the leaf. The linear gradient levels
316 off towards the bulk due to increasing flow mixing effects with the bulk water. In the gas
317 film and leaf tissue the concentration is almost uniform across the thickness. The
318 presented profile in Figure 4 resembles well those discussed in Pedersen *et al.* (2009) who
319 also presented profiles for rice leaves without a gas film. Removal of the gas film

decreased leaf pO_2 from 18.2 ± 0.3 kPa (s.e., n = 6) to 14.0 ± 0.4 kPa (s.e., n = 3) and thus had increased the overall resistance to O_2 flow into the leaf by a factor of about 2.8 (Pedersen *et al.* 2009). However, it should be noted that in Pedersen *et al.* (2009) the DBL was 400 µm with a gas film and 175 µm without. With the thinner DBL on top of the gas film, the leaf pO_2 is expected to be higher than 19 kPa; and the resistance ratio could reasonably increase to a value above 5.

The dimensions of the gas film and DBL from these measurements were used in the subsequent model calculations to investigate the role in leaf O_2 uptake of the gas film together with the influences of stomatal opening, DBL thickness and bulk medium O_2 concentration. Model outputs were compared with results obtained experimentally. Figure 5 shows the results of gas diffusion simulations with the rice leaf model for the case of 5 kPa O_2 in the bulk water and the relatively high cuticle permeability of 3.45×10^{-7} m s^{-1}. The large fluxes into the open stomata, plotted by vectors and colour contours, are evident in the case when a gas film is present. In the absence of a gas film, such high fluxes through stomata are not evident.

Regardless of the used value of the cuticle permeability, in the case of leaves with a gas film and fully open stomata, the total O_2 flow through the stomata is more than 10 times larger than through the cuticle, even though the stomata represent less than 1% of the surface area. Furthermore, if the stomata are almost closed (apertures at 5% of the maximum opening), the stomata still account for at least 5 times more O_2 flow than the entry across the cuticle. In any case, with the gas film present, the total fluxes for fully

343 open and almost closed (5% of the maximum opening) stomata are the same and in both
344 cases substantially higher than when stomata are closed.
345
346 If the leaf lacks a gas film, the flow through fully open stomata reduces significantly
347 depending on the permeability of the cuticle and the bulk pO_2. A curvilinear profile
348 develops above the stomata (Figure 5 (left bottom) and Figure S3) that indicates an added
349 resistance in the DBL above the stomata due to the imbalance of slow O_2 supply through
350 water and relatively faster O_2 removal through air of the open stomata into the tissue, so
351 that a larger local O_2 depletion gradient develops adjacent to stomata when the gas film is
352 absent. This added profile extends about 50 µm into the water layer as evidenced in Figure
353 S3. The result is that the benefit of the stomatal opening for O_2 supply is significantly
354 reduced. Without gas film and when the stomata are almost closed, the total flow through
355 the stomata can even be considerably smaller than that through the cuticle, unless the
356 cuticle has very low permeability (~1.0×10^{-8} m s^{-1}).
357
358 As described above, the changes in O_2 flow are significant for the various pO_2 profiles, as
359 influenced by presence or absence of gas film and whether stomata are closed or open; the
360 O_2 fluxes are plotted in Figure 5 (for a relatively high cuticle permeability). These data
361 demonstrate that gas connectivity between the surface film and the stomatal cavity is
362 essential to provide O_2 for respiration in the leaf in limiting conditions when bulk water
363 pO_2 is below 10 kPa. Without a gas film, total fluxes are significantly smaller.
364
365 Figure 6 (relatively high cuticle permeability) and Figure 7 (low cuticle permeability)
366 graph the calculated profile of O_2 concentration across the DBL, gas film and into the leaf

for different cases of stomatal opening, presence or absence of gas film and O_2 concentration in the water (21 kPa simulating day time concentration, 5 kPa simulating night time). The steady state diffusion profile of O_2 in the DBL linearly decreases towards the gas film and leaf due to the respiratory consumption inside the leaf. The model does not include flow mixing effects, so presents an idealized situation of that observed. Nevertheless, the model captures the major features of O_2 concentration profiles and fluxes in the DBL and gas film covered leaf during dark respiration. Inside the gas film the concentration is uniform due to high gas diffusivity of O_2. When stomata are completely closed a sharp gradient exists across the cuticle that has poor permeability for O_2. When stomata are open and a gas film is present, no gradient exists across the cuticle due to the ensured connectivity of the gas film to the substomatal cavity inside the leaf that is connected to the porous mesophyll. In this condition, even a small opening of the stomata (viz. 5% of maximum aperture) is sufficient to provide aeration of the leaf. For a gas film on a more permeable cuticle ($P_{O_2,g} = 3.45 \times 10^{-7}$ m s^{-1}), with complete closing of the stomata, the internal pO_2 of the leaf drops from 17.5 to 12.9 kPa at 21 kPa bulk water O_2, and from 1.9 to 0.2 kPa at 5 kPa bulk water O_2. For a low cuticle permeability (1.0×10^{-8} m s^{-1}), when stomata fully close, the corresponding internal pO_2 of the leaf drops to 0 kPa for either bulk water O_2 at 5 kPa or even 21 kPa.

When the gas film is absent and the cuticle reasonably permeable, the internal pO_2 of the leaf slightly decreases with closure of the stomata, without reaching hypoxic conditions in either 21 kPa or 5 kPa bulk water. However, if the cuticle is impermeable for O_2, internal pO_2 drops quickly to hypoxic levels even with partial closure of the stomata, with values

as low as 0.02 kPa at 21 kPa O_2 in the bulk water. In any case, the gas film will increase internal pO_2 when stomata are open (even partially), but not when fully closed.

Cuticle permeability affects O_2 profiles on submerged leaves with (almost) closed stomata

The results presented so far are for two divergent parameter values of cuticle permeability taken from studies of other species as data are lacking for rice. Sensitivity of the results with respect to the permeability value is required in order to assess model performance with respect to potential differences with practice. In supplementary material, we elaborate this study by making a comparison of effective permeability values between 1×10^{-8} and 1×10^{-6} m s^{-1}: values that are representative of cuticles ranging from aerial leaves of *Citrus aurantium* L. (Lendzian & Kertiens 1991) to submerged aquatics such as *Potamogeton crispus* (Frost-Christensen *et al.* 2003). Figure S1 shows that no differences are found in pO_2 profiles for leaves with open stomata and a gas film. When a gas film is not present, the result becomes more sensitive to cuticle permeability, but the range of leaf pO_2 remains within the experimental range (Figure S2), at least at high bulk water O_2. The corresponding profiles across the cuticle and stomatal opening are given in Figure S3. Even for the very small cuticle permeability of 1×10^{-8} m s^{-1}, with open stomata tissue pO_2 levels remain higher than 10 kPa at 21kPa bulk water O_2. When stomata could be completely closed, the results obviously become very sensitive to cuticle permeability (Figure S4), because then diffusion across the cuticle is the way O_2 must enter the leaf, albeit a high resistance path. Also for almost closed stomata (Figure S5), the resulting profile is more significantly affected by cuticle permeability than for fully open stomata, with near 0 kPa of O_2 for very small cuticle permeability (Figure S6).

414

415 **Model validation**

416 We found a variation in internal pO_2 between 12.5 and 16.5 kPa (depending on cuticle
417 permeability and a DBL of 185 µm, Figure S3) for open stomata on leaves without a gas
418 film present, agreeing well with measurements of 14 ±0.4 kPa (mean ± SE, n=3) on rice
419 leaves presented in Pedersen *et al.* (2009) for 21 kPa bulk water O_2. When a gas film is
420 present, the internal pO_2 remains at levels above 17 kPa comparing well to measurements,
421 identifying an internal pO_2 of 18.2 ± 0.3 (mean ± SE, n=6) in submerged rice leaves with
422 gas film (Pedersen *et al.* 2009). These leaves, however, had a DBL thickness of about 400
423 µm and higher tissue pO_2 is expected at smaller DBL thickness.

424

425 **The diffusive boundary layer limits O_2 uptake of submerged leaves**

426 The DBL appears to be an important component of the resistance for O_2 supply to the
427 submerged leaf (Figures 6 and 7). The DBL thickness decreases with increasing velocity
428 of the flow (Gundersen & Jørgensen 1990). Here the effect of DBL thickness on leaf O_2
429 flux and tissue pO_2 was calculated.

430

431 Figures 8 and 9 give the leaf O_2 flux and tissue O_2 concentration as a function of the
432 thickness of the DBL for high cuticle permeability. Figures 10 and 11 present the
433 corresponding plots for the low cuticle permeability case. The plots are presented for
434 different stomatal openings, 21 kPa and 5 kPa bulk water pO_2 and with or without gas
435 film. At high (i.e. 21 kPa) bulk water pO_2 (plots (a), (c) and (e)in Figures 8 and 10), the
436 respiratory flux is not limited by the DBL, regardless of the presence of a gas film or
437 stomatal opening. Tissue O_2 levels are above 10 kPa (except for low cuticle permeability

and closed stomata) but do reduce linearly with increasing DBL thickness (plots (a), (c) and (e) in Figures 9 and 11). With the presence of a gas film, the tissue O_2 level increases, indicating a rise in O_2 conductance from the water-to-leaf due to the presence of a gas film. There is also an effect of the stomatal opening: by decreasing the stomatal opening, the increase in leaf tissue pO_2 is larger. When stomata are closed, the gas film has no effect.

At 5 kPa bulk water O_2, the leaf flux decreases with increasing DBL thickness (plots (b), (d) and (f) in Figures 8 and 10). With a gas film present, the effect of DBL thickness is significantly reduced by having open stomata. Again, there is no effect of the gas film on leaves with closed stomata. Associated with the drop in O_2 flux with increased DBL thickness, an exponential drop of tissue pO_2 is observed (plots (b), (d) and (f) in Figures 9 and 11). Without a gas film, clear differences in tissue pO_2 are obtained for different stomatal opening. With a gas film, tissue pO_2 substantially increases, even for the slightest (i.e., 5% of maximum aperture) stomatal opening. More pronounced effects are seen when the cuticle permeability is low.

Increase in resistance due to absence of a gas film

Figure 12 summarizes the respiratory flux response of the leaves to bulk water pO_2 that clearly shows the beneficial effect of the gas film on increasing fluxes in O_2 limiting conditions. With increasing DBL thickness, such as in poorly-mixed still waters, the gain diminishes due to the larger resistance of the DBL. The effect of gas films is more pronounced on leaves with less permeable cuticles.

With the model, the resistance ratio (Eq. 7) is calculated to quantify the reduction in O_2 flux due to absence of a gas film. Figure 13 presents the ratio for leaves with a permeable and impermeable cuticle, respectively, comparing almost closed and open stomata for different DBL thickness. The effects are most spectacular in well mixed waters (represented by a DBL of 90 µm) and almost closed stomata: the resistance then increases with a factor of more than 20 upon removal of the gas film. With fully open stomata, the ratio is between 1.8 and 5. The less permeable the cuticle, the more is gained from the presence of a gas film.

Discussion

We used a 3D model with an idealized geometrical representation of a rice leaf to unravel the importance of gas films on pO_2 profiles and respiration fluxes to submerged rice leaves. The advantage of the approach lies in the fact that parameters that are difficult to control in experiments can be manipulated and consequences evaluated in a comprehensive model of the underwater leaf system. By changing the relevant parameters in realistic value ranges we were able to test what is the contributory effect of the gas film on leaf O_2 uptake during dark respiration, as well as identify the effects of the DBL thickness, cuticle permeability and stomatal opening on O_2 fluxes and tissue pO_2. We found up to a 22-fold reduction in resistance due to presence of a gas film using the model, depending on open area of the stomata, DBL thickness and cuticle permeability. For fully open stomata, a ratio up to 5 was found. This is consistent with earlier work in which the gas films were experimentally removed from leaves of wetland plants such as rice (5-fold; Pedersen *et al.* 2009), *Phragmites australis* (4-fold; Colmer & Pedersen 2008b) and *Phalaris arundinacea* (3-fold; Pedersen & Colmer 2012). We obtained a

significant effect of cuticle permeability, stomatal opening and DBL thickness on the rate of the O_2 uptake in presence of a gas film. These effects indicate that even when gas films are present, differences in underwater O_2 uptake could indeed be observed between species (e.g., with differences in stomatal geometry and distribution, cuticle permeability, leaf morphology influencing DBL), in addition to possible differences in their respiratory demand. Furthermore, the experimental setup used to measure O_2 consumption rates by tissues also influences the result as differences in bulk water flow velocity will affect DBL thickness. Finally, in the measured profiles of submerged leaves with or without gas films, tissue pO_2 was never close to 0 kPa (Figure 4 present paper and Pedersen et al. 2009). We, however, calculated that this condition could happen with closed stomata even at bulk water pO_2 of 21 kPa. Therefore, it is unlikely that full closure of stomata occurs in reality, even when leaves are submerged in darkness, given the model outputs and previous measurements on tissue pO_2 and O_2 consumption rates by submerged leaves of rice in the dark (Figure 4 present paper and Pedersen *et al.* 2009).

Measured leaf segment-in-water respiration rate decreased with decreasing O_2 concentration in the bulk water, following Michaelis-Menten kinetics with an apparent K_{M,O_2} value of > 1 kPa (Figure 3). The model also resulted in response curves of respiration fluxes (i.e. tissue O_2 consumption rate) with apparent K_{M,O_2} values that were significantly larger than the respiratory K_m value (0.0108 kPa of isolated mitochondria, (Millar *et al.* 1994)) used in the model (Figure 12). The exact shape of the curves and the resulting apparent K_{M,O_2} value strongly depend on the presence of a gas film, DBL thickness and cuticle permeability, demonstrating the important contribution of physical resistances to O_2 entry in determining an apparent K_{M,O_2} at a tissue level. As the DBL

parameters are not available for the leaf segments measured in the stirred respiratory chambers, direct comparison of modelled to measured O_2 consumption response curves is therefore not possible. For parameter combinations with gas film, the model overestimates the respiration rate, while for cases without gas film it underestimates the observed respiration rate of leaf segments (data in Pedersen et al., 2009). However, the results indicate that an O_2 diffusion limitation may exist for submerged leaf respiration (Ho *et al.* 2010; Armstrong & Beckett 2011a). Our approach to modelling respiration is simplified by using a Michaelis-Menten model, assuming cytochrome C oxidase as the limiting enzyme and using a K_{M,O_2} value of mitochondria. Such an approach has proven appropriate for many applications (Ho *et al.* 2009; Ho *et al.* 2010; Ho *et al.* 2011; Ho *et al.* 2012; Verboven *et al.* 2012; Verboven *et al.* 2013). For dense tissues such as those of fruits, it has been shown that the effective K_{M,O_2} of tissue can be larger (Lammertyn *et al.* 2001) because of the diffusion limitations inside the tissue. Determination of an effective tissue value is not trivial and is not available for leaves of rice, but the approach taken here has nevertheless been appropriate for this analysis of the effect of gas films on leaves. However it is recognized that the respiration profiles in Figure 9 may not fully comply with the slope of the measured curves, and an alternative K_{M,O_2} value may be more appropriate. In addition, some work has elaborated on different mechanisms that might cause variation in respiration (Zabalza *et al.* 2009), although this is still under debate (Armstrong & Beckett 2011a; Armstrong & Beckett 2011b; ; Nikoloski & van Dongen 2011).

The large resistance of both the cuticle (2.86×10^6 to 1×10^8 s m^{-1}) and the DBL (1.95×10^6 s m^{-1} for a DBL thickness of 185 µm) can limit respiratory gas exchange resulting in

534 the observed respiration response of submerged leaves. This analysis highlights the
535 importance of these resistances, even in the case of the thin (116 µm) lamina of rice leaves
536 and even though no internal pO_2 gradients were calculated in the leaf tissue (Figure 6). In
537 comparison to the cuticle and DBL, the gas film has a negligible resistance (27.9 s m^{-1} for
538 60 µm gas layer thickness). It should be noted that in the experiments (Figure 3), a slight
539 pO_2 gradient was observed in the tissue that was not found in the model outputs. This can
540 be attributed to the fact that in reality the tissue diffusivity for O_2 may differ from the
541 value used in the model calculations. Indeed, here it was assumed that pore connectivity
542 was large and thus not limiting aeration through the pores in the tissue. In reality, O_2
543 diffusivity could be significantly lowered by a limited connectivity of perhaps at least a
544 portion of the pores in plant tissues, specifically if porosity is small such as measured here
545 for the rice leaves. To compute the effect of pore connectivity on tissue diffusivity, one
546 would require 3D imaging (e.g., as done for some other plant tissues, Ho *et al.* 2011;
547 Verboven *et al.* 2012; Verboven *et al.* 2013).
548
549 Leaf lamina porosity (5%, Table 1) was small compared to values previously reported for
550 leaves of rice (Hanba *et al.* 2004; Scafaro *et al.* 2011; Edwards 2013), but here we
551 excluded the mid-rib that has large lacunae (Colmer & Pedersen 2008a). However, even
552 with this small porosity the internal pO_2 was found to be uniform. It is assumed here that
553 tissue diffusivity scales linearly with porosity, neglecting effects of tortuosity (Pham *et al.*
554 2009). As a result, relatively high values of tissue diffusivity are already obtained.
555 Therefore, increasing porosity will not affect the present results because the tissue
556 concentration is already uniform, which shows that even at small porosity the O_2 diffusion
557 in the mesophyll is not limiting within these thin, viz. 116 µm, lamina of rice leaves.

The current work verified that in limiting O_2 conditions in floodwaters, the presence of a gas film reduces the resistance to O_2 entry into submerged leaves, under the condition that stomata are at least partly open, such that the gas film connects to the substomatal cavity. In this manner, the plant avoids the need for O_2 to transverse the large resistance of the cuticle. When gas films are present, O_2 abundantly equilibrates at the large water-gas film interface, then diffusing fast to and across the stomata and into the leaf. In the absence of the surface gas layer, less than 1% of the leaf area (the stomatal opening) is available for gas-water equilibration. This is too small to be effective and an additional gradient develops in the water layer close to the stomata (Figure 5, Figure S1 and Figure S2), as a result of slow diffusion in the aqueous DBL and the oblique (i.e., longer) diffusion paths when leaves lack a gas film, confirming the suggestion by Armstrong, Turner & Beckett (in Colmer *et al.* 2014). We showed also that the magnitude of the stomatal opening between 5% to 100% aperture in leaves with a gas film present does not affect the resulting respiratory flux and leaf pO_2; rather the fact that the aeration pathway is connected via even only slightly opened stomata is important. On the other hand, full stomatal closure will largely negate the beneficial effects of leaf gas films on underwater gas exchange, as then O_2 would need to enter across the large resistance of the cuticle. Finally, the thickness of the gas film did not influence the instantaneous O_2 fluxes and tissue pO_2 (data not shown); however, gas film thickness might influence the persistence of the gas film during longer-term submergence.

Diurnal fluctuations of O_2 in the floodwater can result in hypoxic conditions at dawn following a night period where net O_2 uptake has occurred due to system respiration

582 (Setter *et al.* 1988). During the day, the O_2 produced by underwater photosynthesis by
583 plants and microalgae can again raise the O_2 concentration that peaks in the late afternoon
584 (Ram *et al.* 1999; Winkel *et al.* 2013). Within the base of rice roots Winkel *et al.* (2013)
585 measured the root pO_2 response to changes in bulk water pO_2 and found root pO_2 declined
586 to very low concentrations (0.24 kPa) and was strongly correlated with floodwater pO_2
587 that reached 5 kPa at minimum towards the end of the dark period. At that O_2 level of 5
588 kPa in the floodwater, the present result show that, even with gas film and fully open
589 stomata, leaf pO_2 in still (i.e., non-turbulent) water can drop to values as low as 0.33 kPa.
590 Leaf pO_2 is always higher than the root pO_2, which is expected due to the added diffusion
591 resistance of the internal aeration pathway and respiration in the rice plants. If the
592 floodwater circulates well around the plants, leaf O_2 will be closer to the bulk water O_2
593 level by reducing the DBL thickness. The effect of this on rice root aeration at 23°C was
594 shown in (Armstrong *et al.* 1994). For the realistic experimental condition observed in our
595 experiment, the DBL thickness was 185 µm, resulting in leaf pO_2 equal to 2 kPa at a bulk
596 water O_2 of 5 kPa. Thus, the importance of the DBL on gas exchange to submerged leaves
597 is demonstrated here, with some rice field situations also briefly discussed in Colmer *et al.*
598 (2014); practices that increase water flow will enhance the beneficial effects of gas films
599 on leaves for underwater gas exchange and thus plant tissue O_2 status.
600
601 The presented approach and results, using relevant leaf anatomy parameters and a
602 mechanistic description of O_2 diffusion and consumption in the dark, allowed us to verify
603 and explain the function of stomata, cuticle permeability, gas film and DBL for improving
604 underwater respiration of leaves of rice plants. The approach can be further elaborated for
605 other species, as well as for exploring underwater photosynthesis. For the latter, it will be

606 important to include more detailed models of the tissue anatomy and photosynthesis
607 kinetics (Ho *et al.* 2012).
608
609 **Acknowledgements**
610 Dennis Konnerup and Jenjira Mongon kindly assisted with plant culturing and Dennis
611 Konnerup also conducted the microscopy on leaf surface imprints to assess stomata.
612 Funding by the Danish Research Council Grant No. 09-072482 and the Centre for Lake
613 Restoration, a Villum Kann Rasmussen Centre of Excellence, and the hosting of Ole
614 Pedersen at UWA by the Institute of Advanced Studies, are gratefully acknowledged. The
615 authors thank the Research Council of the K.U. Leuven (OT 12/055) and the Research
616 Fund Flanders (project G.0645.13) for financial support.
617

618 **References**

619

620 Armstrong W. (1979) Aeration in higher plants. *Advances in Botanical Research* **7**, 225-
621 332.
622 Armstrong W. & Beckett P.M. (2011a) Experimental and modelling data contradict the
623 idea of respiratory down-regulation in plant tissues at an internal [O_2] substantially
624 above the critical oxygen pressure for cytochrome oxidase. *New Phytologist* **190**,
625 431-441.
626 Armstrong W. & Beckett P.M. (2011b) The respiratory down-regulation debate. *New*
627 *Phytologist* **190**, 276-278.
628 Armstrong W., Brändle R. & Jackson M.B. (1994) Mechanisms of flood tolerance in
629 plants. *Acta Botanica Neerlandica* **43**, 307-358.
630 Bailey-Serres J. & Voesenek L.A.C.J. (2008) Flooding stress: Acclimations and genetic
631 diversity. *Annual Review of Plant Biology* **59**, 313-339.
632 Beckett P.M. & Armstrong W. (1992) The modelling of convection and diffusion-driven
633 aeration in plants. In: *Oxygen transport in biological systems* (eds S. Egginton &
634 H.F. Ross), pp. 253-293. Cambridge University Press, Cambridge.
635 Caird M.A., Richards J.H. & Donovan L.A. (2007) Nighttime stomatal conductance and
636 transpiration in C_3 and C_4 plants. *Plant Physiology* **143**, 4-10.
637 Colmer T.D., Armstrong W., Greenway H., Ismail A.M., Kirk G.J.D. & Atwell B.J.
638 (2014) Physiological mechanisms of flooding tolerance in rice: transient complete
639 submergence and prolonged standing water. *Progress in Botany* **75**, 255-307.
640 Colmer T.D. & Pedersen O. (2008a) Oxygen dynamics in submerged rice (*Oryza sativa*).
641 *New Phytologist* **178**, 326-334.

642 Colmer T.D. & Pedersen O. (2008b) Underwater photosynthesis and respiration in leaves
643 of submerged wetland plants: gas films improve CO_2 and O_2 exchange. *New*
644 *Phytologist* **177**, 918-926.
645 Colmer T.D., Winkel A. & Pedersen O. (2011) A perspective on underwater
646 photosynthesis in submerged terrestrial wetland plants. *AoB PLANTS* **2011**, plr030.
647 Edwards G.E. (2013) Gas exchange and leaf structure in genus *Oryza*. *Plant Physiology*,
648 doi:10.1104/pp.1113.217497.
649 Frost-Christensen H., Jørgensen L.B. & Floto F. (2003) Species specificity of resistance to
650 oxygen diffusion in thin cuticular membranes from amphibious plants. *Plant, Cell*
651 *& Environment* **26**, 561-569.
652 Gundersen J.K. & Jørgensen B.B. (1990) Microstructure of diffusive boundary layers and
653 the oxygen uptake of the sea floor. *Nature* **345**, 604-607.
654 Hanba Y.T., Shibasaka M., Hayashi Y., Hayakawa T., Kasamo K., Terashima I. &
655 Katsuhara M. (2004) Overexpression of the barley aquaporin HvPIP2;1 increases
656 internal CO_2 conductance and CO_2 assimilation in the leaves of transgenic rice
657 plants. *Plant Cell Physiology* **45**, 521-529.
658 Ho Q.T., Verboven P., Mebatsion H.K., Verlinden B., Vandewalle S. & Nicolaï B. (2009)
659 Microscale mechanisms of gas exchange in fruit tissue. *New Phytologist* **182**, 163-
660 174.
661 Ho Q.T., Verboven P., Verlinden B.E., Herremans E., Wevers M., Carmeliet J. & Nicolaï
662 B.M. (2011) A three-dimensional multiscale model for gas exchange in fruit. *Plant*
663 *Physiology* **155**, 1158-1168.

Ho Q.T., Verboven P., Verlinden B.E., Schenk A., Delele M.A., Rolletschek H., Vercammen J. & Nicolaï B.M. (2010) Genotype effects on internal gas gradients in apple fruit. *Journal of Experimental Botany* **61**, 2745-2755.

Ho Q.T., Verboven P., Yin X., Struik P.C. & Nicolaï B.M. (2012) A microscale model for combined CO_2 diffusion and photosynthesis in leaves. *Plos One* **7**, e48376.

Ishihara K., Nishihara T. & Ogura T. (1971) *The relationship between environmental factors and behaviour of stomata in the rice plant. 1. on the measurement of the stomatal aperture*. Paper presented at the Crop Sci Soc Japan Proc.

Jørgensen B.B. & Revsbech N.P. (1985) Diffusive boundary layers and the oxygen uptake by sediments and detritus. *Limnology and Oceanography* **30**, 111-122.

Lammertyn J., Franck C., Verlinden B.E. & Nicolaï B.M. (2001) Comparative study of the O_2, CO_2 and temperature effect on respiration between 'Conference' pear cells in suspension and intact pears. *Journal of Experimental Botany* **52**, 1769-1777.

Lendzian K.J. (1982) Gas permeability of plant cuticles. *Planta* **155**, 310-315.

Lendzian K.J. & Kertiens g. (1991) Sorption and transport of gases and vapors in plant cuticles. *Reviews of Environmental Contamination and Toxicology* **121**, 65-128.

Lide D.R. (1999) *Handbook of chemistry and physics*. CRC Press, New York.

Maberly S.C. & Madsen T.V. (2002) Freshwater angiosperm carbon concentrating mechanisms: processes and patterns. *Functional Plant Biology* **29**, 393-405.

Matsuo T., Kumazawa K., Ishii R., Ishihara K. & Hirata H. (1995) *Science of the rice plant*. Food and Agriculture Policy Research Center.

Millar A.H., Bergersen F.J. & Day D.A. (1994) Oxygen affinity of terminal oxydases in soybean mitochondria. *Plant Physiology and Biochemistry* **32**, 847-852.

687 Mommer L., Pedersen O. & Visser E.J.W. (2004) Acclimation of a terrestrial plant to
688 submergence facilitates gas exchange under water. *Plant, Cell & Environment* **27**,
689 1281-1287.
690 Mommer L. & Visser E.J.W. (2005) Underwater photosynthesis in flooded terrestrial
691 plants: A matter of leaf plasticity. *Annals of Botany* **96**, 581-589.
692 Nielsen S.L. & Sand-Jensen K. (1989) Regulation of photosynthetic rates of submerged
693 rooted macrophytes. *Oecologia* **81**, 364-368.
694 Nikoloski Z. & van Dongen J.T. (2011) Modeling alternatives for interpreting the change
695 in oxygen-consumption rates during hypoxic conditions. *New Phytologist* **190**,
696 273-276.
697 Pedersen O. & Colmer T.D. (2012) Physical gills prevent drowning of many wetland
698 insects, spiders and plants. *Journal of Experimental Biology* **215**, 705-709.
699 Pedersen O., Colmer T.D. & Sand-Jensen K. (2013) Underwater photosynthesis of
700 submerged plants – recent advances and methods. *Frontiers in Plant Science* **4**,
701 Pedersen O., Rich S.M. & Colmer T.D. (2009) Surviving floods: leaf gas films improve
702 O_2 and CO_2 exchange, root aeration, and growth of completely submerged rice.
703 *The Plant Journal* **58**, 147-156.
704 Pedersen O., Vos H. & Colmer T.D. (2006) Oxygen dynamics during submergence in the
705 halophytic stem succulent *Halosarcia pergranulata*. *Plant Cell and Environment*
706 **29**, 1388-1399.
707 Pham Q., Bulens I., Ho Q.T., Verlinden B.E., Verboven P. & Nicolaï B.M. (2009)
708 Simultaneous measurement of ethane diffusivity and skin resistance of 'Jonica'
709 apples by efflux experiment. *Journal of Food Engineering* **95**, 471-478.

710 Ram P.C., Singh A.K., Singh B.B., Singh V.K., Singh H.P., Setter T.L., Singh V.P. &
711 Singh R.K. (1999) Environmental characterization of floodwater in eastern India:
712 relevance to submergence tolerance of lowland rice. *Experimental Agriculture* **35**,
713 141-152.
714 Raskin I. (1983) A method for measuring leaf density, thickness and internal gas.
715 *Hortscience* **18**, 698-699.
716 Raskin I. & Kende H. (1983) How does deep water rice solve its aeration problem? *Plant*
717 *Physiology* **72**, 447-454.
718 Sage T.L. & Sage R.F. (2009) The functional anatomy of rice leaves: implications for
719 refixation of photorespiratory CO_2 and efforts to engineer C_4 photosynthesis into
720 rice. *Plant and Cell Physiology* **50**, 756-772.
721 Sand-Jensen K., Pedersen O., Binzer T. & Borum J. (2005) Contrasting oxygen dynamics
722 in the freshwater isoetid *Lobelia dortmanna* and the marine seagrass *Zostera*
723 *marina*. *Annals of Botany* **96**, 613-623.
724 Scafaro A.P., von Caemmerer S., Evans J.R. & Atwell B.J. (2011) Temperature response
725 of mesophyll conductance incultivated and wild *Oryza* species with contrasting
726 mesophyll cell wall thickness. *Plant, Cell & Environment* **34**, 1999-2008.
727 Schneider C.A., Rasband W.S. & Eliceiri K.W. (2012) NIH Image to ImageJ: 25 years of
728 image analysis. *Nature Methods* **9**, 671-675.
729 Sculthorpe C.D. (1967) *The biology of aquatic vascular plants*. Edward Arnold Ltd.,
730 London.
731 Setter T.L., Kupkanchanakul T., Waters I. & Greenway H. (1988) Evaluation of factors
732 contributing to diurnal changes in O_2 concentrations in floodwater of deepwater
733 rice fields. *New Phytologist* **110**, 151-162.

734 Setter T.L., Waters I., Wallace I., Bekhasut P. & Greenway H. (1989) Submergence of
735 rice. I. Growth and photosynthetic response to CO_2 enrichment of floodwater.
736 *Australian Journal of Plant Physiology* **16**, 251-263.
737 Smart R. & Barko J. (1985) Laboratory culture of submersed freshwater macrophytes on
738 natural sediments. *Aquatic Botany* **21**, 251-263.
739 Thomson C.J., Armstrong W., Waters I. & Greenway H. (1990) Aerenchyma formation
740 and associated oxygen movement in seminal and nodal roots of wheat. *Plant, Cell*
741 *& Environment* **13**, 395-403.
742 Verboven P., Herremans E., Borisjuk L., Helfen L., Ho Q.T., Tschiersch H., Fuchs J.,
743 Nicolaï B.M. & Rolletschek H. (2013) Void space inside the developing seed of
744 *Brassica napus* and the modelling of its function. *New Phytologist*,
745 Verboven P., Pedersen O., Herremans E., Ho Q.T., Nicolaï B.M., Colmer T.D. & Teakle
746 N. (2012) Root aeration via aerenchymatous phellem: three-dimensional micro-
747 imaging and radial O_2 profiles in *Melilotus siculus*. *New Phytologist* **193**, 420-431.
748 Waters I., Armstrong W., Thompson C., Setter T., Adkins S., Gibbs J. & Greenway H.
749 (1989) Diurnal changes in radial oxygen loss and ethanol metabolims in roots of
750 submerged and non-submerged rice seedlings. *New Phytologist* **113**, 439-451.
751 Widawsky D.A. & O'Toole J.C. (1990) Prioritizing the rice research agenda for Eastern
752 India. In: *Rice research in Asia: progress and priorities* (eds R.E. Evenson, R.V.
753 Herdt, & M. Hossain), pp. 109-129. International Rice Research Institute, Los
754 Baños.
755 Winkel A., Colmer T.D., Ismail A.M. & Pedersen O. (2013) Internal aeration of paddy
756 field rice (*Oryza sativa* L.) during complete submergence – importance of light and
757 floodwater O_2. *New Phytologist* **197**, 1193-1203.

Winkel A., Colmer T.D. & Pedersen O. (2011) Leaf gas films of *Spartina anglica* enhance rhizome and root oxygen during tidal submergence. *Plant, Cell & Environment* **34**, 2083-2092.

Zabalza A., Van Dongen J.T., Froehlich A., Oliver S.N., Faix B., Gupta K.J., Schmälzlin E., Igal M., Orcaray L. & Royuela M. (2009) Regulation of respiration and fermentation to control the plant internal oxygen concentration. *Plant Physiology* **149**, 1087-1098.

Zeigler R.S. & Puckridge D.W. (1995) Improving sustainable productivity in rice-based rainfed lowland systems of South and Southeast Asia. *GeoJournal* **35**, 307-324.

772 Table 1. Morphological, diffusion and respiration parameters of submerged leaves of rice
773 (*Oryza sativa*). Where values were not from own measurements, references are given in
774 footnotes.

	Own measurements (mean ± st. dev.)	Model
Leaf morphology		
lamina leaf thickness (µm)	116.0 ± 3.0	116.0
porosity of lamina (%)	3.4 ± 1.6	5.0
porosity of mesophyll tissue (%)		2.0
epidermis thickness (µm) [a]		10.0
stomatal density adaxial surface (mm^{-2}) [b]	268 ± 64	239
stomatal density abaxial surface (mm^{-2}) [b]	294 ± 66	239
axial distance between stomata (µm)	49.6 ± 6.2	49.0
lateral distance between stomata (µm)	84.4 ± 13.6	84.0
stomatal opening width, 100% open (µm) [c]		1.1
stomatal opening width, 5% open (µm) [c]		1.1
stomatal opening length, 100% open (µm)	16.3 ± 2.6	14.0
stomatal surface area, 100 % open ($µm^2$)		15.4
stomatal surface area, 5 % open ($µm^2$)		0.8
area fraction stomata, 100% open (%)		0.37
area fraction stomata, 5% open (%)		0.0185
stomatal cavity radius (µm) [a]		13.0

Diffusion and respiration properties		
diffusive boundary layer thickness (µm)	185	90 / 185 / 370
gas film thickness (µm)	60	60
O_2 partial pressure (kPa)		2.5 / 5 / 10 / 21
O_2 concentration in air (mol m^{-3})		8.33 / 3.97 / 1.98 / 0.99
O_2 concentration in water (mol m^{-3})		0.288 / 0.137 / 0.069 / 0.034
O_2 diffusion coefficient in air at 30°C, $D^a_{O_2,g}$ (m^2 s^{-1}) [d]		2.15×10^{-5}
O_2 diffusion coefficient in water at 30°C, $D^w_{O_2,l}$ (m^2 s^{-1}) [d]		2.75×10^{-9}
O_2 diffusion coefficient of epidermis at 30°C, $D^w_{O_2,l}$ (m^2 s^{-1}) [d]		2.75×10^{-9}
effective O_2 diffusion coefficient in mesophyll tissue at 30°C, $D^t_{O_2,g}$ (m^2 s^{-1}) [e]		4.3×10^{-7}
effective cuticle permeability, $P_{O_2,g}$ (m s^{-1}) [f]		1.0×10^{-8} to 1.0×10^{-6}
maximum respiration rate, $V_{\max,O_2}$ (mol m^{-3} s^{-1}) [g]		0.012
mitochondrial Michaelis-Menten constant, K_{M,O_2} (kPa) [h]		0.0108
Henry constant for oxygen, H_{O_2} (mol m^{-3} kPa^{-1})		0.01371
universal gas constant, R (J K^{-1} mol^{-1})		8.314
Temperature, T (°C)		30°C

[a] Estimated from micrographs presented in Sage & Sage (2009).

[b] Stomatal density was also measured by Matsuo *et al.* (1995), who obtained values between 150 and 650 per mm² depending on leaf age.

[c] Ishihara *et al.* (1971) observed a variation in stomatal aperture that varies between 0.5 and 1.2 µm. Here it is assumed that partial closure of the stomata reduces the aperture to a small central area between the guard cells, rather than a reduced slit width over the length, which could cause numerical errors in the model.

[d] Calculated from Lide (1999).

[e] Calculated as the product of tissue porosity and the O_2 diffusion coefficient in air (30°C), assuming connectivity of the gas-filled spaces in the tissue.

[f] Estimated from ranges provided in Lendzian (1982), Lendzian & Kertiens (1991) and Frost-Christensen *et al.* (2003).

[g] Obtained from measured respiration curve in Figure 3 by transforming the mean area-based $V_{\max,O_2}$ value to a mean volume-based $V_{\max,O_2}$ value using measured lamina thickness.

[h] K_{M,O_2} value for cytochrome C oxidase as taken from Ho *et al.* (2009).

Figure legends

Figure 1. Schematic presentation of different mechanisms of O_2 diffusion to submerged leaves. Upper diagrams present cases where a gas film is present. Two extreme cases are presented: (a) with open stomata, (b) with closed stomata. Two respective cases are given in diagrams (c) and (d) for leaves without gas film. Arrows hypothesize the relative direction and magnitude of O_2 fluxes to the leaf for the different cases.

Figure 2. Simple and stylised diagram of rice (*Oryza sativa*) leaf lamina (left) and corresponding computer model geometry (right) that takes into account observed symmetry in the leaf morphology. All sides of the model geometry are symmetry planes through which O_2 flux is zero, except for the far end of the DBL where the bulk water pO_2 is specified.

Figure 3. Dark respiration rate (expressed on two-sided area) of submerged rice (*Oryza sativa*) leaf lamina segments (gas films present) at various bulk water pO_2, at 30^{o}C. The experimental data were fitted to a Michaelis-Menten model (V_{max} 0.83 ± 0.03 µmol m^{-2} s^{-1}; K_m 3.08 ±0.037 kPa; r^2 0.91; error = SE). The maximum respiration rate corresponds to 0.012 mol O_2 m^{-3} s^{-1}, expressed on a tissue volume basis using leaf dimensions given in Table 1.

Figure 4. O_2 concentration and corresponding pO_2 profile across the gas film and adjacent diffusive boundary layer (DBL) of a submerged leaf of rice (*Oryza sativa*) obtained from microelectrode profiling experiments, at 30^{o}C. Concentrations are expressed in molar

concentration (mmol m^{-3}) and partial pressure (kPa). The box-whiskers plot shows median (horizontal line), 25 and 75% percentiles (box) and minimum and maximum (bars).

Figure 5. Simulations of O_2 diffusion into submerged leaves of rice (*Oryza sativa*). From left to right are plotted results for leaves without gas film, and with gas film and different stomatal opening fractions (100%, 5%, 0%). The simulations are shown for a bulk water O_2 partial pressure (pO_2) of 5 kPa. Two horizontal planes (one at the water-gas film interface and one just above the leaf cuticle) in the top row of figures plot the O_2 diffusion flux perpendicular to the leaf surface. The arrows indicate the direction and relative magnitude of the fluxes on those planes. The middle row of figures present a magnified view of the fluxes (in the perpendicular, or 'normal', direction to the leaf) near the stomata, showing clear differences between the cases. The bottom row of figures are the resulting quasi steady state O_2 concentration profiles expressed as pO_2. Plots are for cuticle permeability equal to 3.45×10^{-7} m s^{-1} (see supplementary Figures S1, S2 and S5 for plots with cuticle permeability equal to 1.0×10^{-8} m s^{-1}).

Figure 6. Effect of presence of a gas film on calculated partial pressure (pO_2) profiles from water to submerged leaves of rice (*Oryza sativa*) for two bulk water O_2 concentrations (21 kPa on the left, 5 kPa on the right). The different cases are for open stomata (a, b), almost closed stomata (c, d) and closed stomata (e, f). (+GF/-GF: with/without gas film, DBL: diffusive boundary layer). The plotted profiles are for a single trace across the cuticle. The profile across the stomatal opening may deviate from this as is shown in supplementary materials (Figures S3 and S6). Profiles are for cuticle permeability equal to 3.45×10^{-7} m s^{-1}. DBL thickness is 185 µm.

839

840 Figure 7. Effect of presence of a gas film on calculated partial pressure (pO_2) profiles from
841 water to submerged leaves of rice (*Oryza sativa*) for two bulk water O_2 concentrations (21
842 kPa on the left, 5 kPa on the right), in the dark. The different cases are for open stomata (a,
843 b), almost closed stomata (c, d) and closed stomata (e, f). (+GF/-GF: with/without gas
844 film, DBL: diffusive boundary layer). The plotted profiles are for a single trace across the
845 cuticle. The profile across the stomatal opening may deviate from this as is shown in
846 Figures S3 and S6. Profiles are for cuticle permeability equal to 1.0×10^{-8} m s^{-1}. DBL
847 thickness is 185 µm.

848

849 Figure 8. Effect of the presence of gas film on calculated O_2 fluxes into submerged leaves
850 of rice (*Oryza sativa*) during dark respiration as a function of bulk water O_2 concentration
851 (21 kPa and 5 kPa O_2) and diffusive boundary layer (DBL) thickness, assuming a
852 relatively high cuticle permeability (3.45×10^{-7} m s^{-1}): (a, b) open stomata, (c, d) almost
853 closed stomata, (e, f) closed stomata. In plots (a), (c), (e) and (f), the flux for with and
854 without gas film are equal and thus symbols cannot be discerned (open symbols confer
855 with closed symbols, thus for e.g. 21 kPa bulk water O_2 and closed stomata, +GF and -GF
856 fluxes are equal). (+GF/-GF: with/without gas film, DBL: diffusive boundary layer).

857

858 Figure 9. Effect of the presence of gas film on calculated tissue O_2 partial pressure (pO_2)
859 of submerged leaves of rice (*Oryza sativa*) during dark respiration as a function of bulk
860 water O_2 concentration (21 kPa and 5kPa O_2) and diffusive boundary layer (DBL)
861 thickness, assuming a relatively high cuticle permeability (3.45×10^{-7} m s^{-1}): (a-b) open
862 stomata, (b-c) almost closed stomata, (d-e) closed stomata. In plots (e) and (f), the pO_2 for

with and without gas film are equal and thus symbols cannot be discerned (open symbols confer with closed symbols, thus for e.g. 21 kPa bulk water O_2 and closed stomata, +GF and -GF pO_2 are equal). (+GF/-GF: with/without gas film, DBL: diffusive boundary layer). .

Figure 10. Effect of the presence of a gas film on calculated O_2 fluxes into submerged leaves of rice (*Oryza sativa*) during dark respiration as a function of bulk water O_2 concentration (21 kPa and 5 kPa O_2) and diffusive boundary layer (DBL) thickness, assuming low cuticle permeability (1.0×10^{-8} m s^{-1}): (a, b) open stomata, (c, d) almost closed stomata, (e, f) closed stomata. In plots (a), (e) and (f), the flux for with and without gas film are equal and thus symbols cannot be discerned (open symbols confer with closed symbols, thus for e.g. 21 kPa bulk water O_2 and closed stomata, +GF and -GF fluxes are equal). (+GF/-GF: with/without gas film, DBL: diffusive boundary layer).

Figure 11. Effect of the presence of a gas film on calculated tissue O_2 partial pressure (pO_2) of submerged leaves of rice (*Oryza sativa*) during dark respiration as a function of bulk water O_2 concentration (21 kPa and 5 kPa O_2) and diffusive boundary layer (DBL) thickness, assuming low cuticle permeability (1.0×10^{-8} m s^{-1}): (a, b) open stomata, (c, d) almost closed stomata, (e, f) closed stomata. In plots (e) and (f), the pO_2 for with and without gas film are equal (open symbols confer with closed symbols, thus for e.g. 21 kPa bulk water O_2 and closed stomata, +GF and -GF pO_2 are equal). (+GF/-GF: with/without gas film, DBL: diffusive boundary layer).

886 Figure 12. Effect of gas films on respiratory O_2 fluxes (µmol m^{-2} s^{-1}) into submerged
887 leaves of rice (*Oryza sativa*) with almost closed stomata (5% open). Plots are given for
888 different diffusive boundary layer (DBL) thickness as a function of bulk water O_2 partial
889 pressure (pO_2) for two cuticle permeability values: 1.0×10^{-8} m s^{-1} (a, c, e) and 3.45×10^{-7}
890 m s^{-1} (b, d, f). (+GF/-GF: with/without gas film, DBL: diffusive boundary layer).
891
892 Figure 13. Increase in resistance for O_2 uptake during dark respiration of submerged
893 leaves of rice (*Oryza sativa*) due to absence of a gas film expressed as the resistance ratio
894 $r_{R_{O_2}}$ of submerged leaves without to ones with gas film as a function of diffusive boundary
895 layer (DBL) thickness, stomatal opening and cuticle permeability: (a) 3.45×10^{-7} m s^{-1}, (b)
896 1.0×10^{-8} m s^{-1}.
897
898 **Supporting information**
899 Supplementary Materials are comprised in a document describing the sensitivity of the
900 simulation results with respect to cuticle permeability including figures presenting
901 additional pO_2 profiles for different values of cuticle permeability.
902

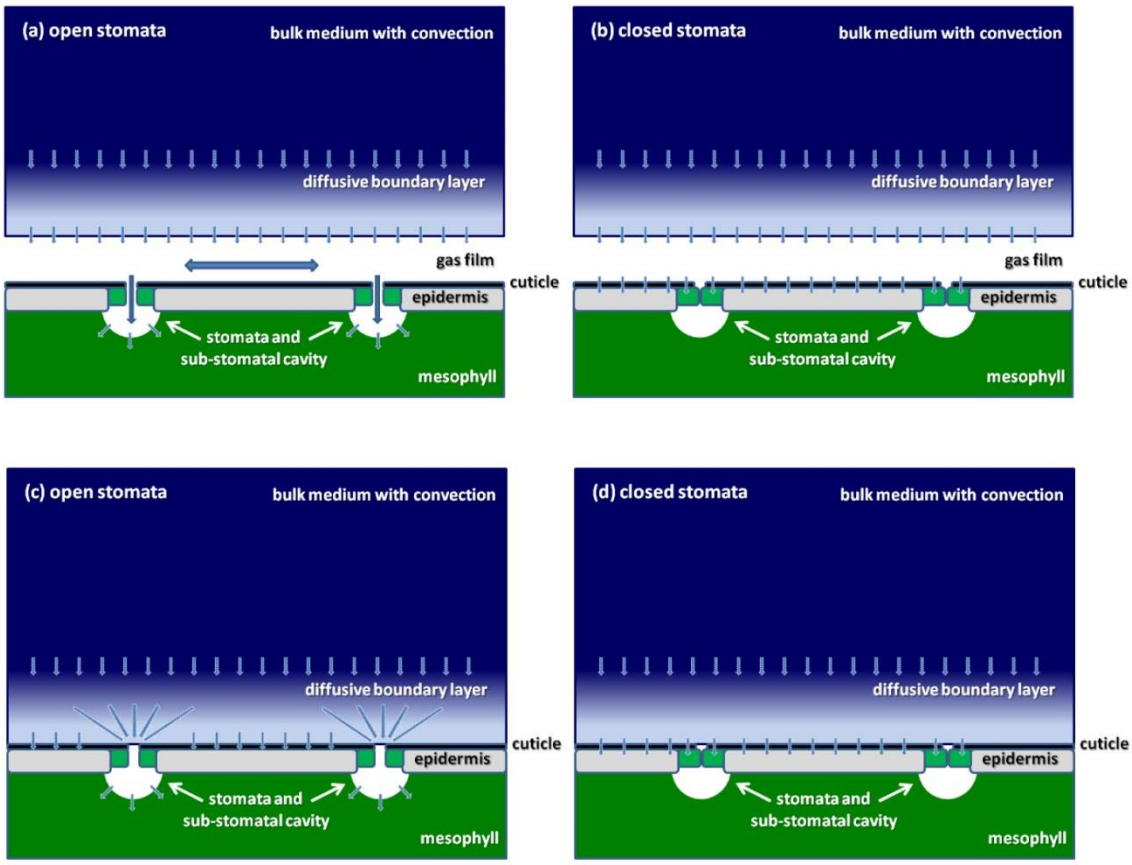

903

904 Figure 1. diffusion mechanism

905

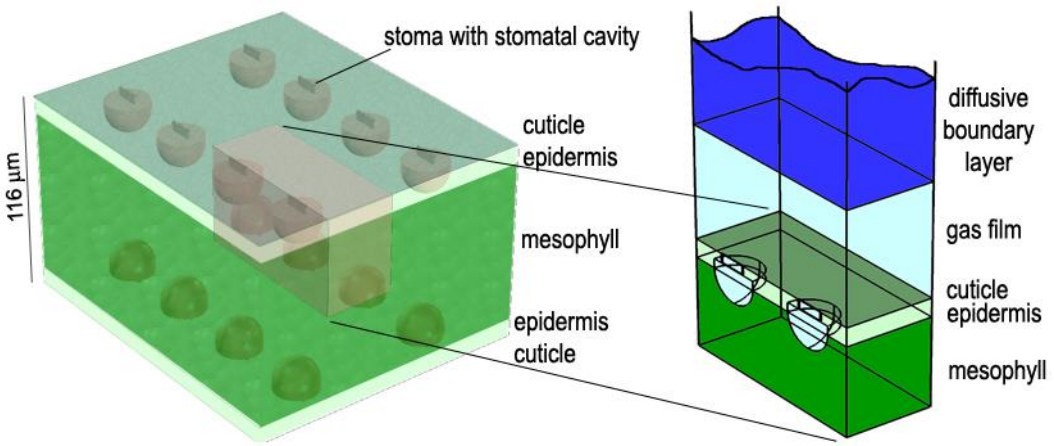

906

907 Figure 2. model geometry for gas diffusion simulation

908

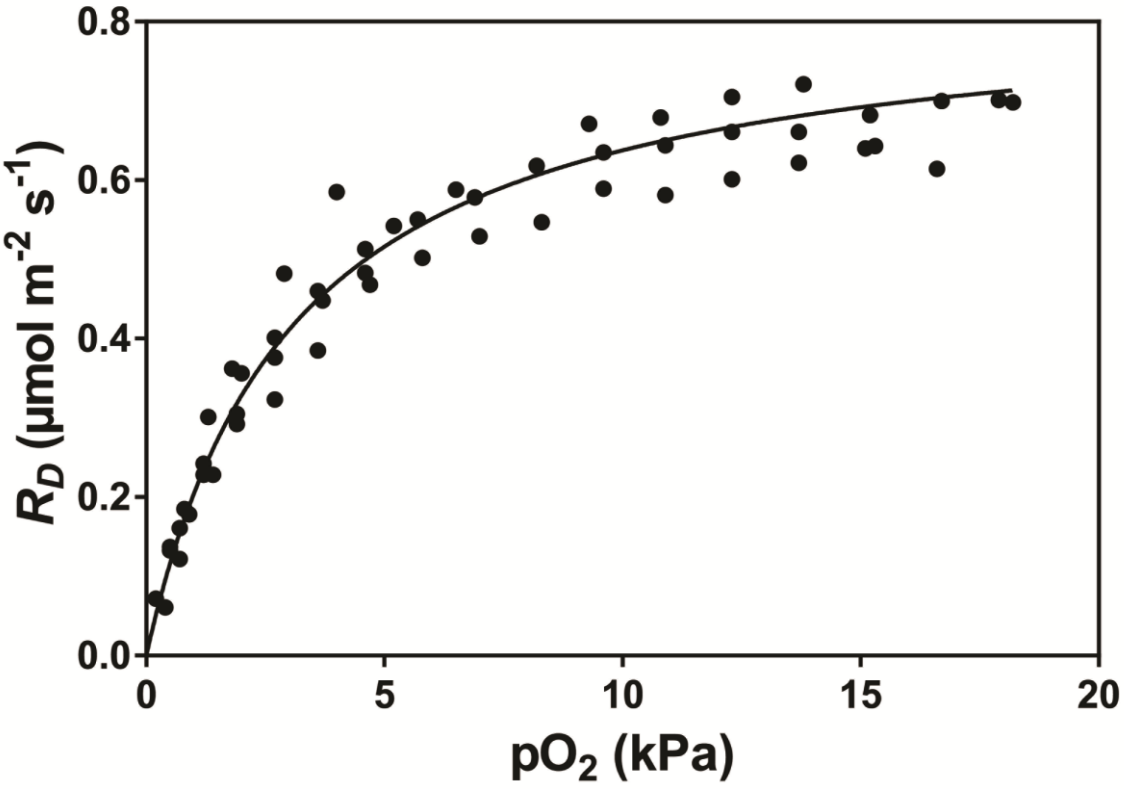

909

910 Figure 3. respiration curve

911

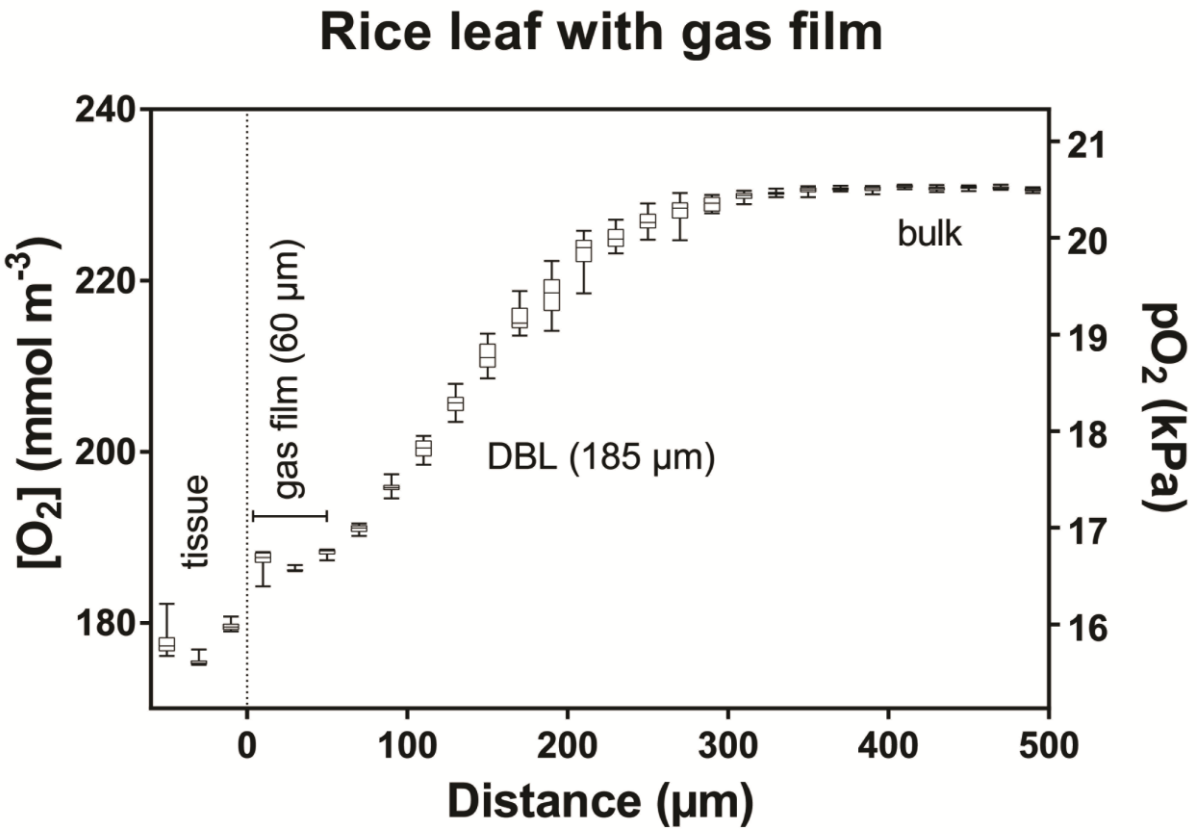

912

913 Figure 4. measured pO_2 profile

914

915

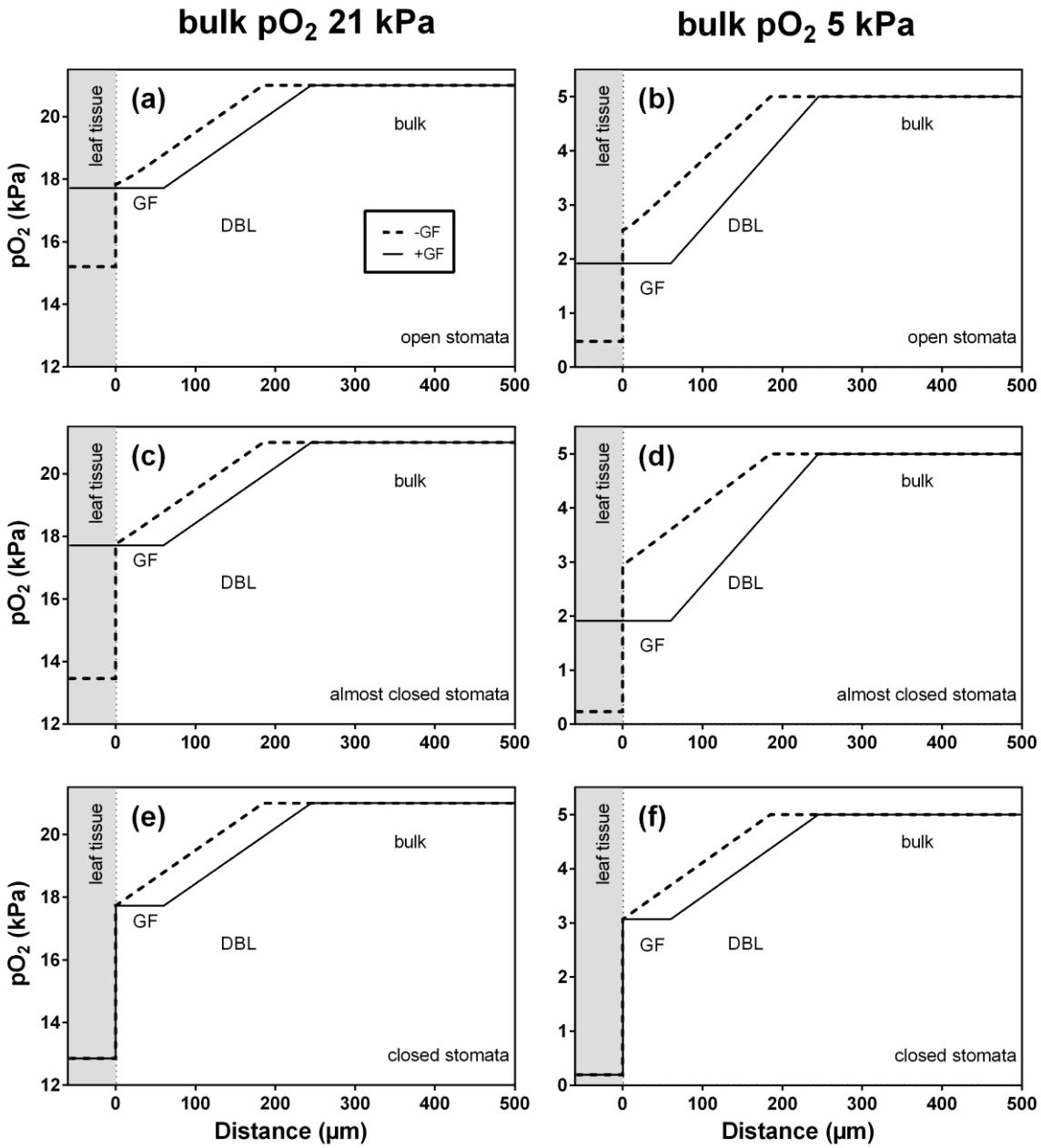

916

917 Figure 6. pO_2 gradients, high cuticle permeability

918

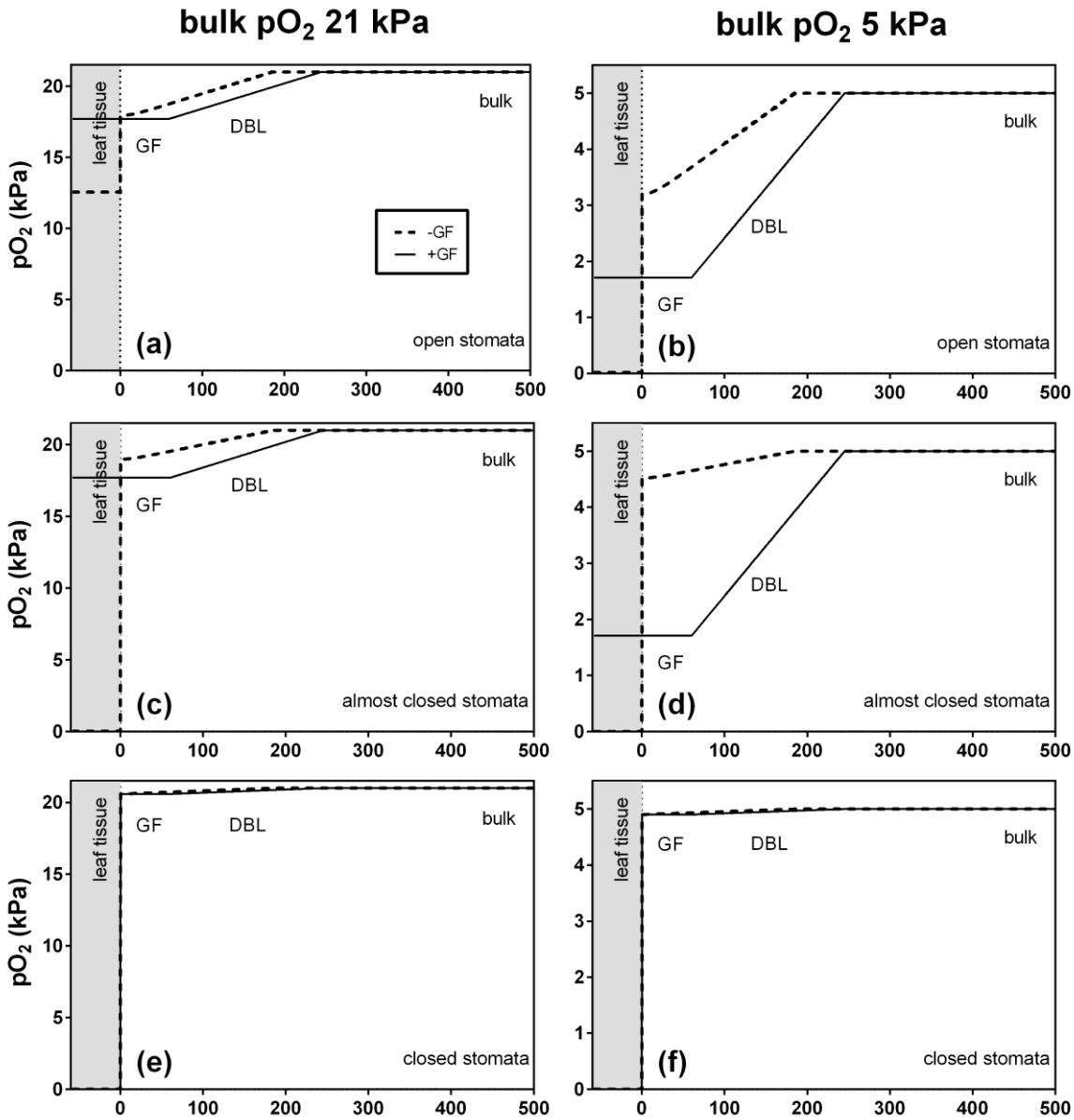

Figure 7. pO_2 gradients, low cuticle permeability

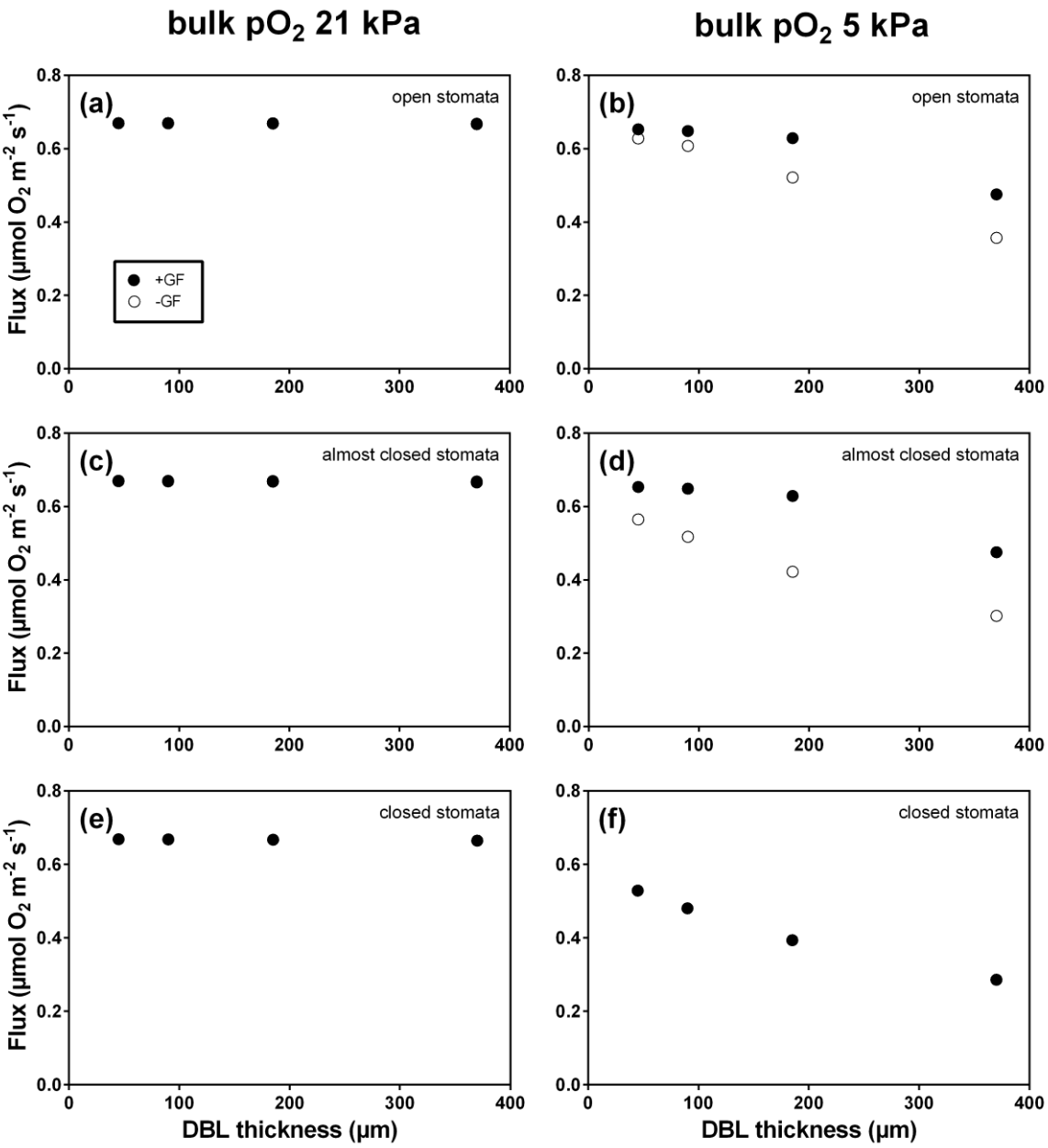

923

924 Figure 8. flux vs. DBL thickness, high cuticle permeability

925

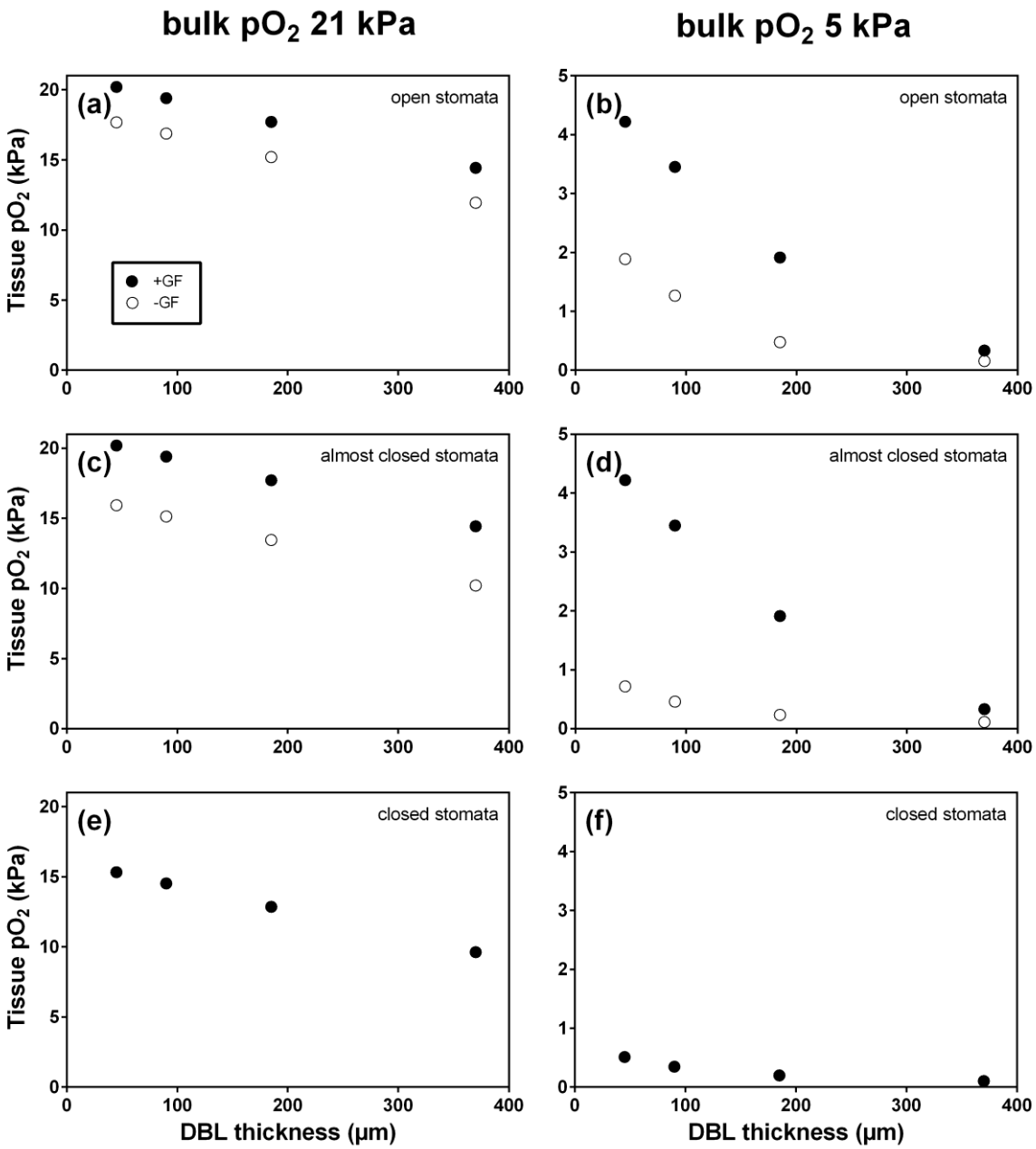

926

927 Figure 9. pO2 vs. DBL thickness, high cuticle permeability

928

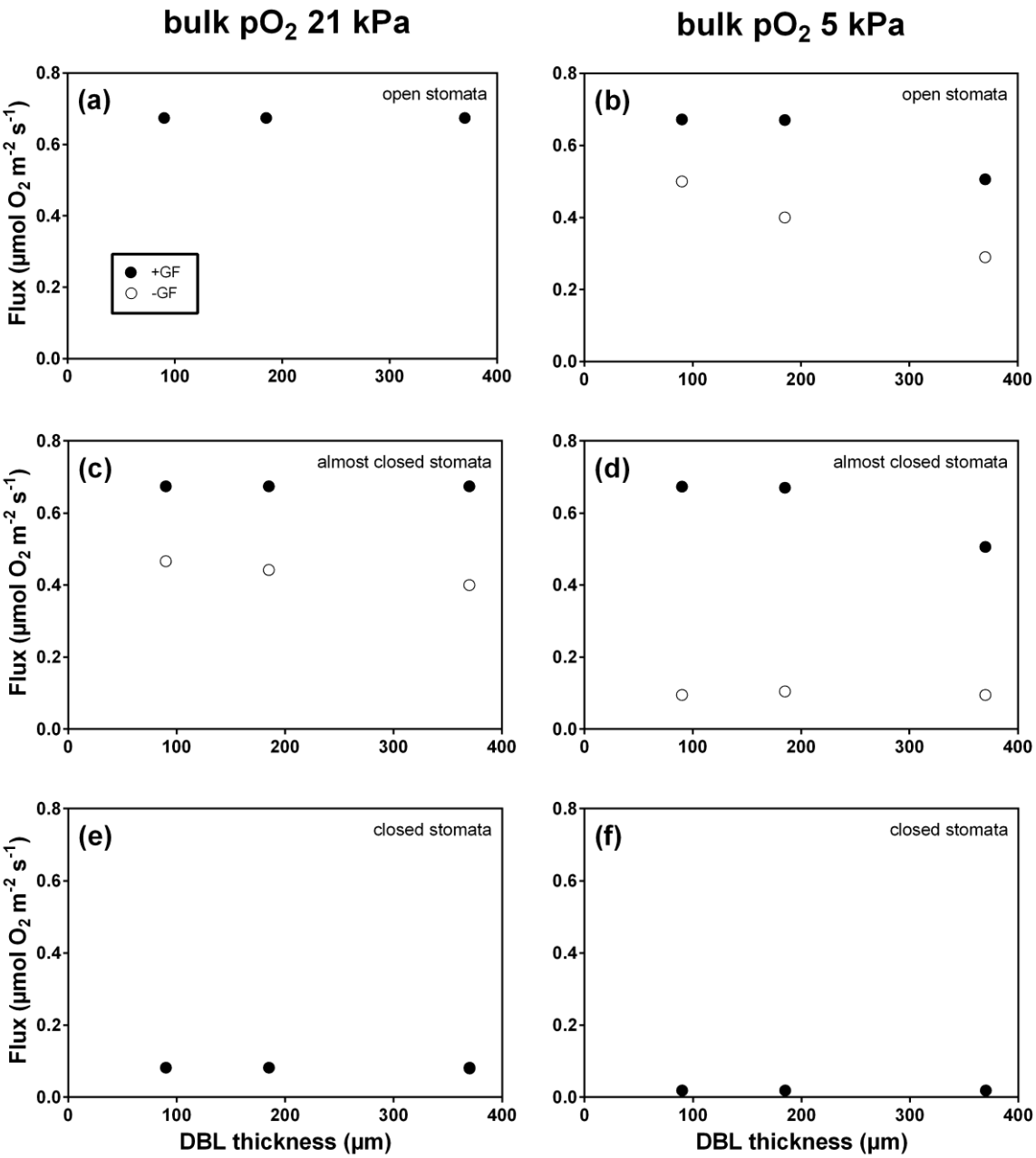

929

930 Figure 10. flux vs. DBL thickness, low cuticle permeability

931

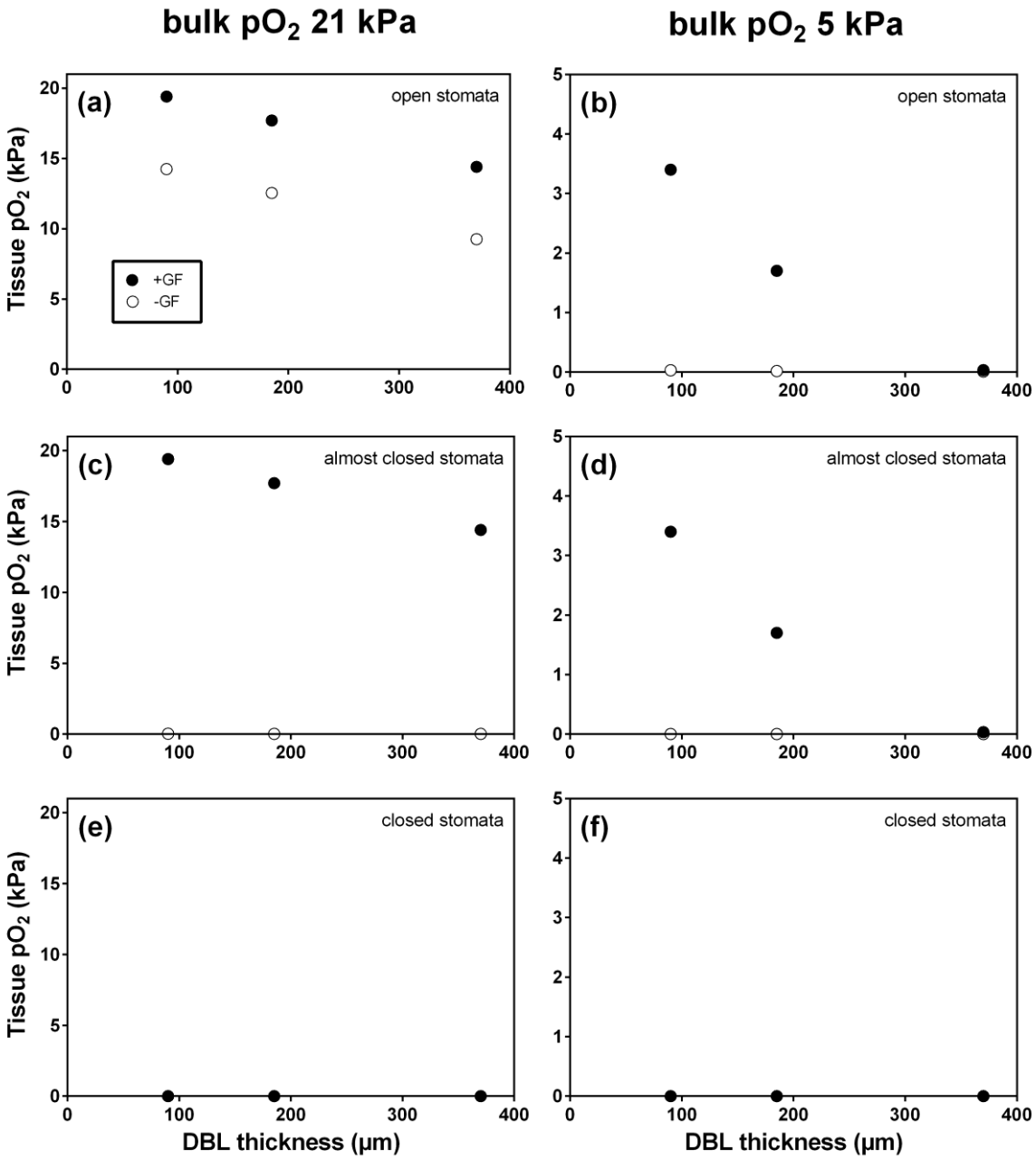

932

933 Figure 11. pO2 vs. DBL thickness, low cuticle permeability

934

935

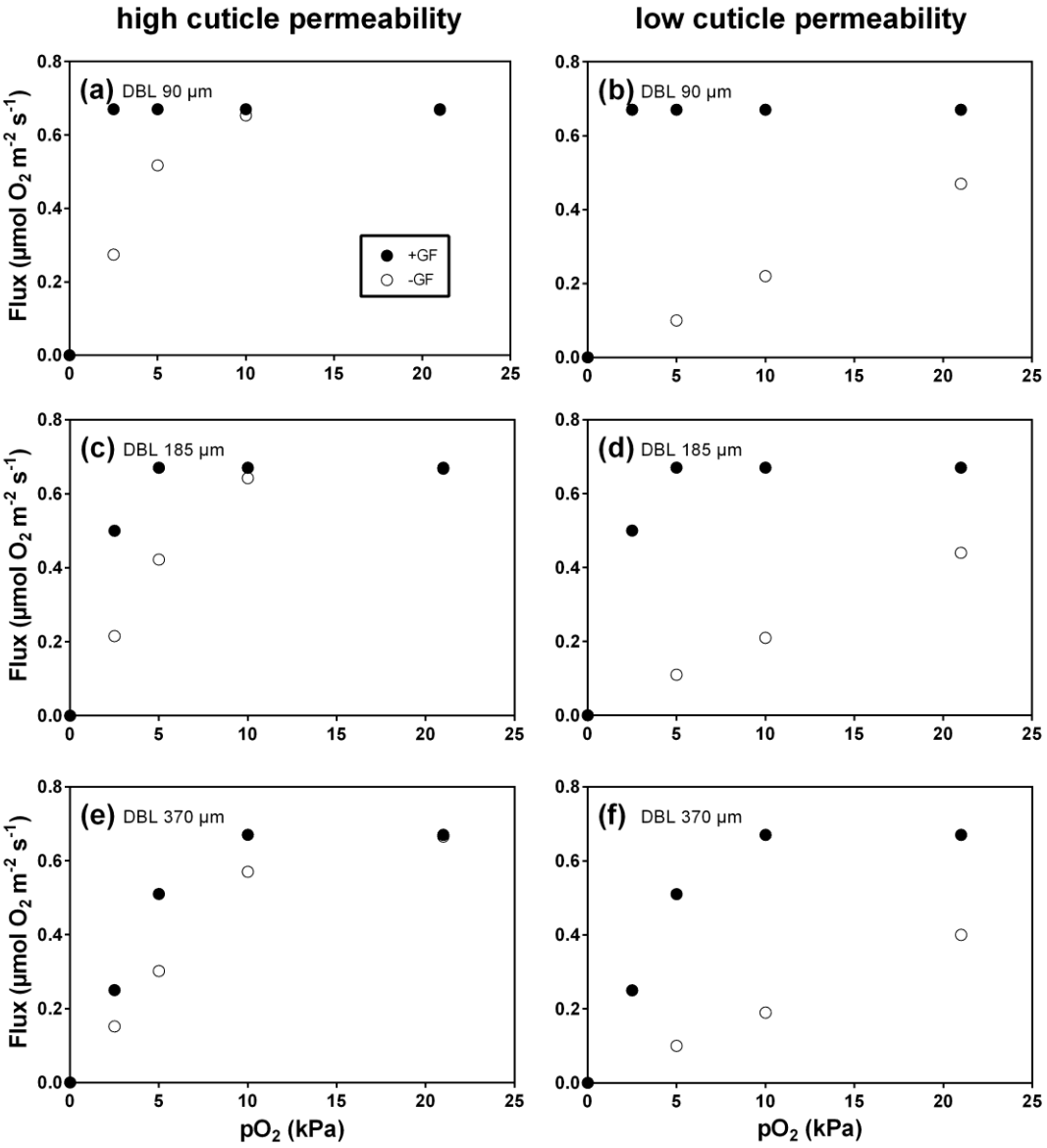

936

937 Figure 12. fluxes for high and low cuticle permeability

938

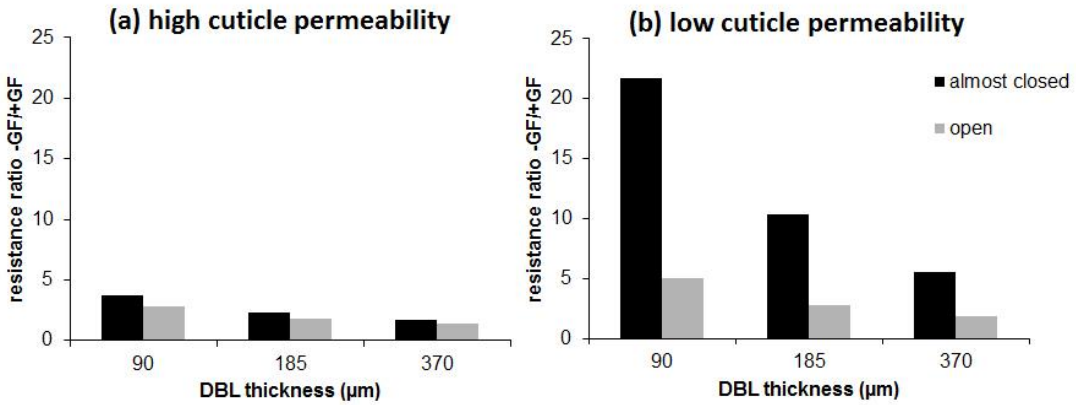

939

940 Figure 13. resistance ratios

941

Supplementary Materials for Verboven *et al.* (2014). The mechanism of improved aeration due to gas films on leaves of submerged rice.

Sensitivity with respect to cuticle permeability

The main body of the text uses an estimate of the cuticle permeability to O_2 at a value of 3.45×10^{-7} m/s based on ranges given in literature (Lendzian, 1982; Lendzian & Kertiens 1991; Frost-Christensen et al., 2003). Here the sensitivity of the model result is assessed with respect to the value of cuticle permeability (P) over a wide range from 1×10^{-8} to 1×10^{-6} m/s. We limit the analysis to the condition of 21 kPa O_2, and consider the cases of fully open and fully closed stomata, and stomata with a small aperture (5% of fully open), and again for a submerged leaf in the dark.

Open stomata

In the case of a submerged leaf with a gas film and open stomata, the cuticle permeability is not relevant to the process (Figure S1). The gas flow occurs only through the stomata and is sufficient to supply the complete leaf with O_2 for unlimiting respiration at V_{max,O_2} (Table 1).

When the gas film is not present while the stomata remain open, the effect of cuticle permeability becomes pronounced in the range simulated. Figure S2 plots the O_2 profiles obtained with the model. As the permeability increases, it approaches the O_2 condition of the leaf with gas film in Figure S1, with high enough O_2 concentrations for maximal respiration. As the cuticle permeability decreases, all O_2 needs to flow to the stoma resulting in distinct gradients at the stoma limiting O_2 supply and consequent decrease of p O_2 inside the leaf.

Over the range of two orders of magnitude for the permeability of the cuticle, we found a variation in internal p O_2 between 12.5 and 16.5 kPa for open stomata on leaves without a gas film present (Figure S3), agreeing well with measurements on rice leaves that revealed leaf pO_2 of 14 ±0.4 kPa (s.e., n=3) (Pedersen et al. 2009). With the value used in the main body of the text, the different features of the profile are captured and could thus be used in the comparative study presented. When a gas film is present, the internal pO_2 remains at higher levels, being above 17 kPa. Again this is consistent with measurements on submerged rice leaves with gas films, for which an internal pO_2 of 18.2 ± 0.3 (s.e., n=6) was found (Pedersen et al. 2009).

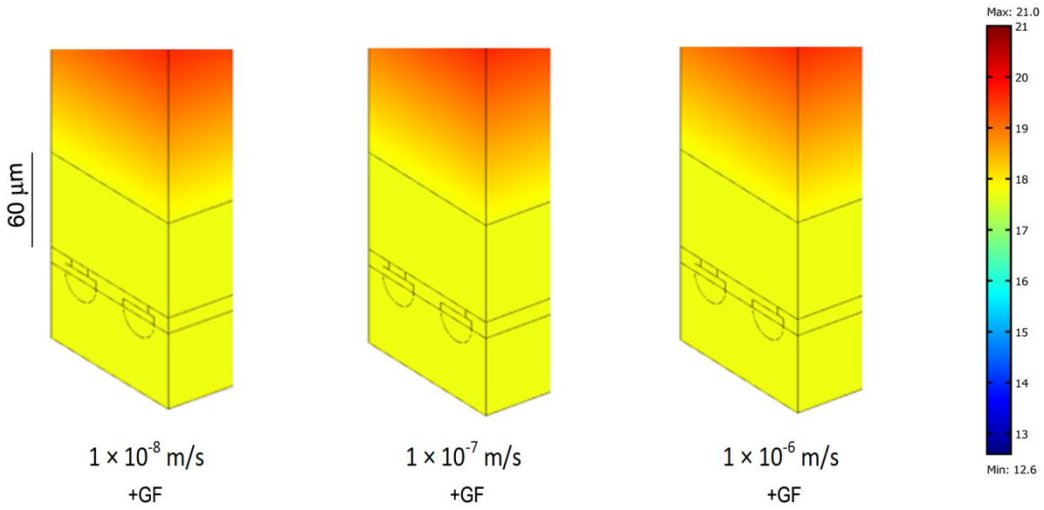

Figure S1. Effect of cuticle permeability and presence of a gas film on calculated partial pressure (pO_2) profiles from water to submerged leaves of rice (*Oryza sativa*) for bulk water O_2 concentration of 21 kPa. Different values of cuticle permeability were used in the presence of a gas film and open stomata. DBL thickness is 185 µm.

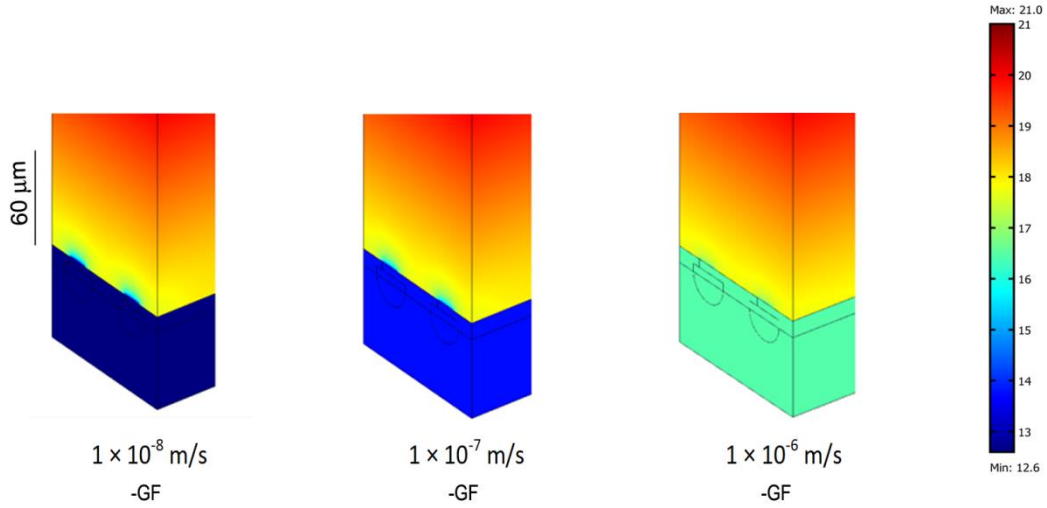

Figure S2. Effect of cuticle permeability and absence of a gas film on calculated partial pressure (pO_2) profiles from water to submerged leaves of rice (*Oryza sativa*) for bulk water O_2 concentration of 21 kPa. Different values of cuticle permeability were used in the absence of a gas film and open stomata. DBL thickness is 185 µm.

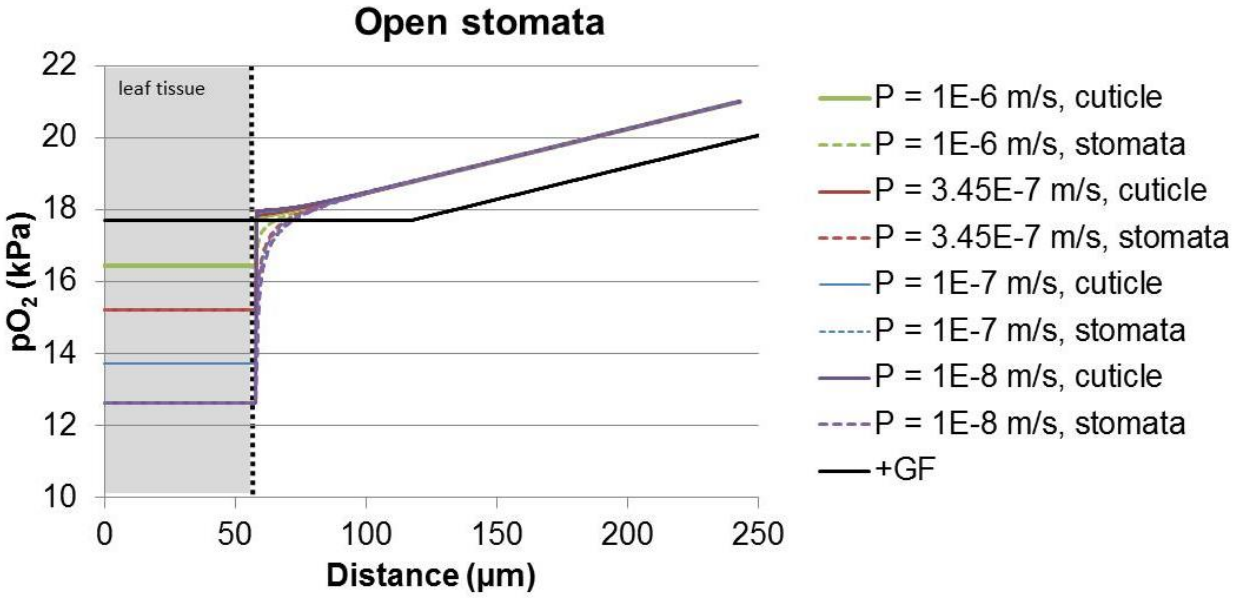

Figure S3. Effect of cuticle permeability (P) and absence of a gas film on calculated partial pressure (pO_2) profiles from water to submerged leaves of rice (*Oryza sativa*) for bulk water O_2 concentration of 21 kPa. The cases presented are for open stomata and different

values of cuticle permeability for a leaf without a gas film. The condition with gas film (+GF) is insensitive to cuticle permeability (Figure S1). Profiles are plotted across the cuticle and across the stomatal opening. DBL thickness is 185 µm.

Closed stomata

For a submerged leaf with completely closed stomata, the effect of cuticle permeability reasonably becomes very important as the cuticle is then the single route for O_2 supply. Figure S4 plots the effect of the cuticle permeability value on the resulting pO_2 profile from water to submerged leaves of rice. In the case of closed stomata; there is also no effect of the presence of a gas film. When the resistance becomes very high ($P = 1 \times 10^{-8}$ m/s), internal pO_2 drops to zero, and O_2 cannot penetrate the leaf and so there is no apparent diffusive boundary layer (DBL).

Clearly the results for closed stomata are much more sensitive to cuticle permeability. The general trend is, however, that internal pO_2 will markedly drop with closure of the stomata, whether a gas film is present or not. The extent of the drop may not be easily assessed and the results in the main body of the text are therefore rather conservative. Depending on the actual cuticle permeability, closed stomata will result in much lower values of tissue pO_2 than described in the main text, as is evidenced here.

Almost closed stomata

In the case of almost closed stomata (Figure S5 and Figure S6), the resulting profiles for leaves without gas films are considerably affected by the cuticle permeability, similar to that of closed stomata.

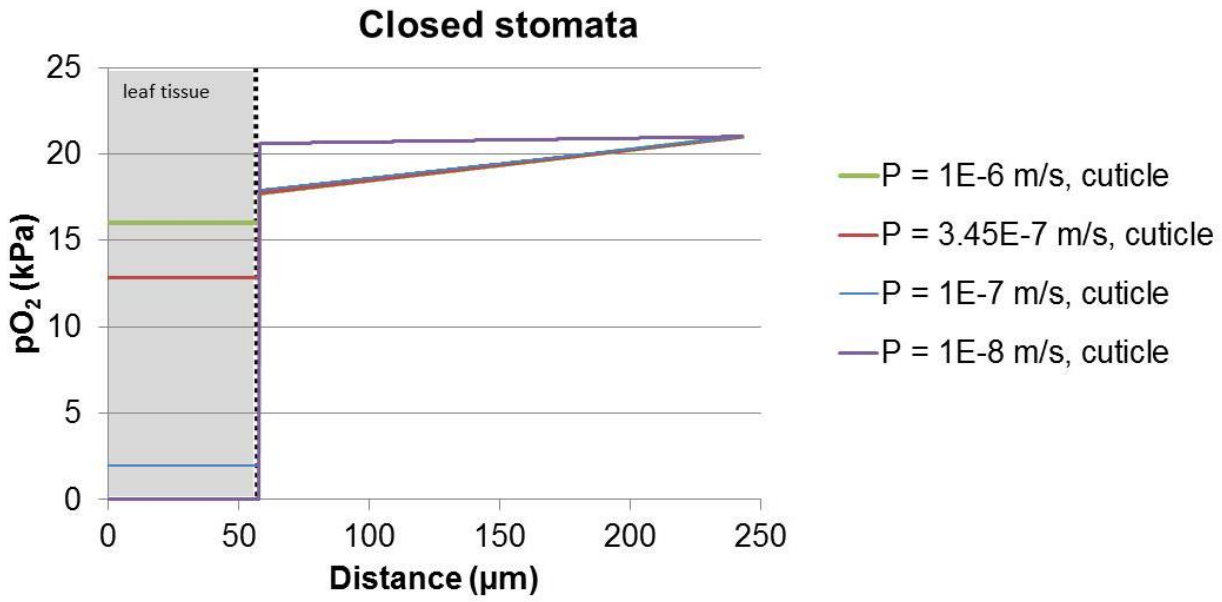

Figure S4. Effect of cuticle permeability (P) and absence of a gas film on calculated partial pressure (pO_2) profiles from water to submerged leaves of rice (*Oryza sativa*) for bulk water O_2 concentration of 21 kPa. The cases are for closed stomata and different values of cuticle permeability without a gas film. The condition with gas film (+GF) is completely analogous. Profiles are plotted across the cuticle. DBL thickness is 185 µm.

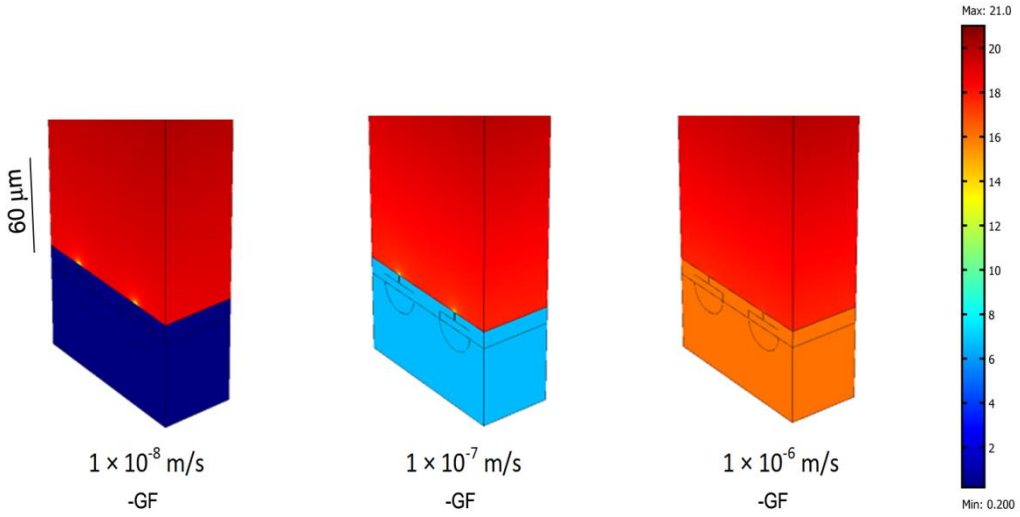

Figure S5. Effect of cuticle permeability and absence of a gas film on calculated partial pressure (pO_2) profiles from water to submerged leaves of rice (*Oryza sativa*) for bulk

water O_2 concentration of 21 kPa. Different values of cuticle permeability were used in the absence of a gas film and almost closed (5% open area) stomata. DBL thickness is 185 µm.

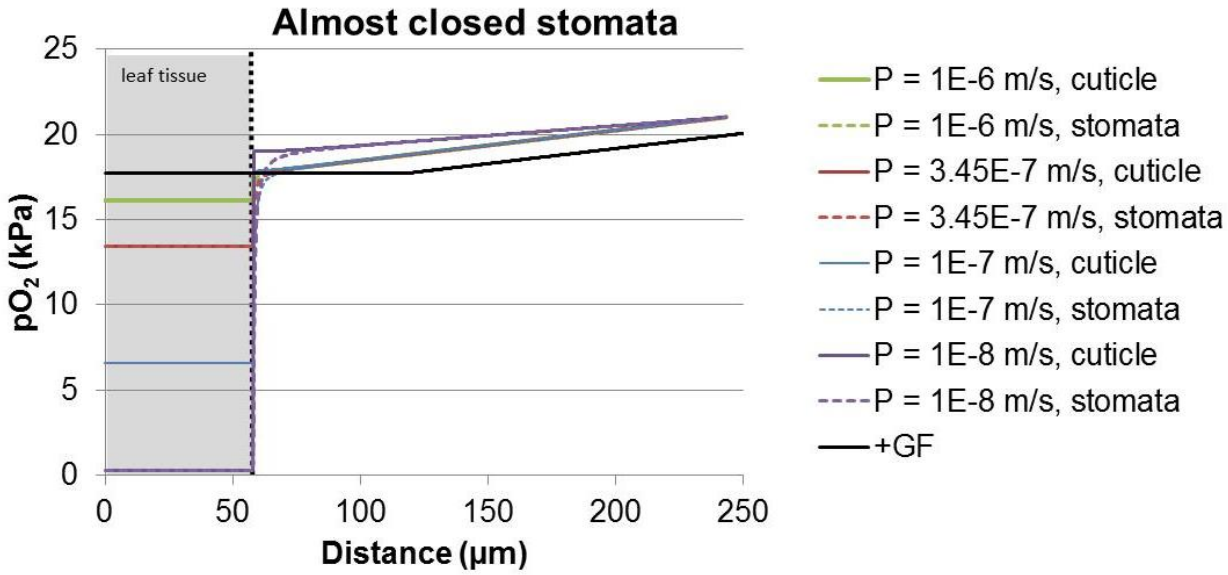

Figure S6. Effect of cuticle permeability (P) and presence of a gas film on calculated partial pressure (pO_2) profiles from water to submerged leaves of rice (*Oryza sativa*) for bulk water O_2 concentration of 21 kPa. The cases are for almost closed stomata (5% open area) and different values of cuticle permeability without a gas film are presented. The condition with gas film (+GF) is insensitive to cuticle permeability. Profiles are plotted across the cuticle and a stomatal opening. DBL thickness is 185 µm.